Neuron

Article

Ketamine induces plasticity in a norepinephrine-astroglial circuit to promote behavioral perseverance

Graphical abstract

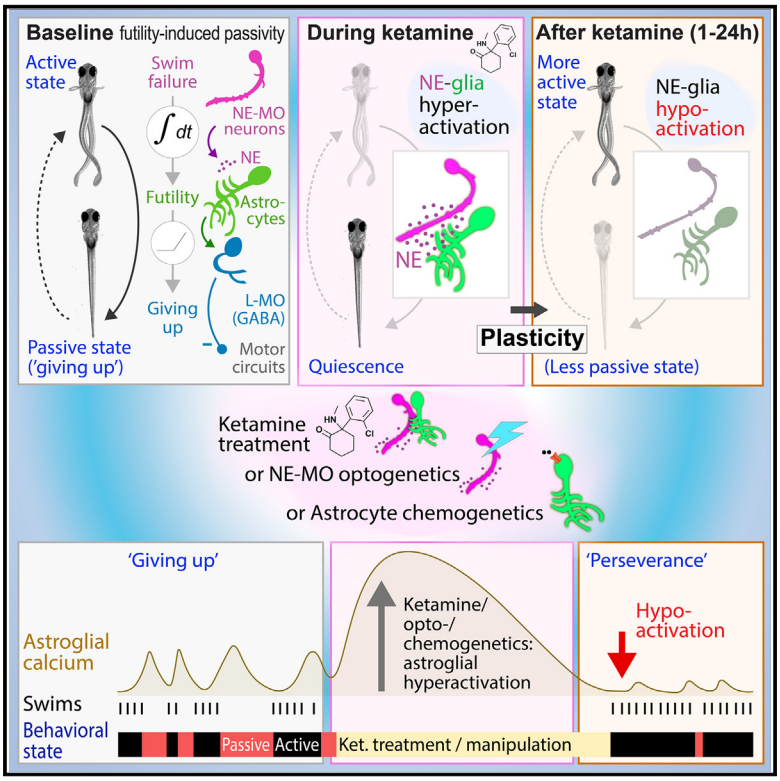

Highlights

- Zebrafish "give up" when behavior is futile, analogous to learned helplessness
- Brief exposure to ketamine causes long-term suppression of giving up
- Ketamine induces plasticity in the NE-astroglial system to enhance perseverance
- Astrocyte activation may be a critical component of ketamine's effects across species

Authors

Marc Duque, Alex B. Chen, Eric Hsu, ..., Mark C. Fishman, Florian Engert, Misha B. Ahrens

Correspondence

mduqueramirez@g.harvard.edu (M.D.), abchen@g.harvard.edu (A.B.C.), ahrensm@janelia.hhmi.org (M.B.A.)

In brief

Duque et al. show that astroglial calcium is recruited at active-to-passive transitions during learned-helplessness-like assays in both zebrafish and mice and that a variety of antidepressant compounds have consistent effects across both species. Ketamine, applied transiently, causes acute norepinephrine-mediated astrocytic hyperactivation followed by prolonged suppression to promote lasting behavioral resilience.

Duque et al., 2025, Neuron *113*, 1–15
February 5, 2025
https://doi.org/10.1016/j.neuron.2024.11.011

CellPress

Neuron

CellPress
OPEN ACCESS

Article

Ketamine induces plasticity in a norepinephrine-astroglial circuit to promote behavioral perseverance

Marc Duque,[1,2,3,17,*] Alex B. Chen,[1,2,3,17,*] Eric Hsu,[4,17] Sujatha Narayan,[3] Altyn Rymbek,[5] Shahinoor Begum,[6,7] Gesine Saher,[8] Adam E. Cohen,[6,7] David E. Olson,[9,10,11,12] Yulong Li,[13,14] David A. Prober,[5] Dwight E. Bergles,[4,15,18] Mark C. Fishman,[16,18] Florian Engert,[1,18] and Misha B. Ahrens[3,18,19,*]

[1]Department of Molecular and Cellular Biology, Harvard University, Cambridge, MA 02138, USA
[2]Graduate Program in Neuroscience, Harvard Medical School, Boston, MA 02115, USA
[3]Janelia Research Campus, Howard Hughes Medical Institute, Ashburn, VA 20147, USA
[4]Solomon H. Snyder Department of Neuroscience, Johns Hopkins University School of Medicine, Baltimore, MD 21205, USA
[5]Tianqiao and Chrissy Chen Institute for Neuroscience, Division of Biology and Biological Engineering, California Institute of Technology, Pasadena, CA 91125, USA
[6]Department of Physics, Harvard University, Cambridge, MA 02138, USA
[7]Department of Chemistry and Chemical Biology, Harvard University, Cambridge, MA 02138, USA
[8]Department of Neurogenetics, Max Planck Institute for Multidisciplinary Sciences, Göttingen 37075, Germany
[9]Department of Chemistry, University of California, Davis, Davis, CA 95616, USA
[10]Department of Biochemistry & Molecular Medicine, School of Medicine, University of California, Davis, Sacramento, CA 95817, USA
[11]Center for Neuroscience, University of California, Davis, Davis, CA 95618, USA
[12]Institute for Psychedelics and Neurotherapeutics, University of California, Davis, Davis, CA 95616, USA
[13]State Key Laboratory of Membrane Biology, Peking University School of Life Sciences, Beijing 100871, China
[14]PKU-IDG/McGovern Institute for Brain Research, Beijing 100871, China
[15]Kavli Neuroscience Discovery Institute, Johns Hopkins University, Baltimore, MD 21205, USA
[16]Department of Stem Cell and Regenerative Biology, Harvard University, Cambridge, MA 02138, USA
[17]These authors contributed equally
[18]These authors contributed equally
[19]Lead contact
*Correspondence: mduqueramirez@g.harvard.edu (M.D.), abchen@g.harvard.edu (A.B.C.), ahrensm@janelia.hhmi.org (M.B.A.)
https://doi.org/10.1016/j.neuron.2024.11.011

SUMMARY

Transient exposure to ketamine can trigger lasting changes in behavior and mood. We found that brief ketamine exposure causes long-term suppression of futility-induced passivity in larval zebrafish, reversing the "giving-up" response that normally occurs when swimming fails to cause forward movement. Whole-brain imaging revealed that ketamine hyperactivates the norepinephrine-astroglia circuit responsible for passivity. After ketamine washout, this circuit exhibits hyposensitivity to futility, leading to long-term increased perseverance. Pharmacological, chemogenetic, and optogenetic manipulations show that norepinephrine and astrocytes are necessary and sufficient for ketamine's long-term perseverance-enhancing aftereffects. *In vivo* calcium imaging revealed that astrocytes in adult mouse cortex are similarly activated during futility in the tail suspension test and that acute ketamine exposure also induces astrocyte hyperactivation. The cross-species conservation of ketamine's modulation of noradrenergic-astroglial circuits and evidence that plasticity in this pathway can alter the behavioral response to futility hold promise for identifying new strategies to treat affective disorders.

INTRODUCTION

The behavior of animals incorporates past experience to adapt to changing environments.[1–5] Importantly, transient perturbations of circuits, such as through emotionally salient events or brief exposure to psychoactive chemicals, can profoundly alter circuit dynamics and behavior far outlasting the input's lifetime. Understanding the cellular and circuit mechanisms by which transient perturbations cause long-lasting changes in circuit dynamics and behavior benefits from an experimental system in which the acute and long-lasting consequences of perturbations can be measured brain-wide during behavior. The larval zebrafish's optical accessibility makes it an ideal system to study such questions,[6,7] as activity in nearly all cells[8] can be

Please cite this article in press as: Duque et al., Ketamine induces plasticity in a norepinephrine-astroglial circuit to promote behavioral perseverance, Neuron (2024), https://doi.org/10.1016/j.neuron.2024.11.011

measured simultaneously while the fish performs fictive behaviors in virtual reality.[9]

Futility-induced passivity is a state-switching behavior based on the larval zebrafish's innate tendency to swim in the direction of optic flow, a position-stabilizing behavior known as the optomotor response (OMR).[10,11] Previously, we showed that when swims become futile (i.e., stop moving the fish forward through virtual reality), fish at first produce higher-vigor swims[12] but eventually stop swimming altogether, akin to "giving up."[9] Futile swims enhance firing of hindbrain noradrenergic neurons, and this noradrenergic signal is integrated over time through intracellular calcium signaling in a population of hindbrain astrocytes to suppress swimming.[9] These studies indicate that there is a noradrenergic-astroglial circuit that integrates information about behavioral futility and induces switching from an active to a passive behavioral state.

Mammals also undergo behavioral state switching and can enter periods of immobility in assays based on inescapable challenge, as observed during forced swim and tail suspension tests.[13,14] Such behavior in mammals, often referred to as passive coping and learned helplessness, can be modulated by ketamine and other compounds.[15–17] Although there are qualitative differences between these mammalian and fish assays, the potential conceptual link provided between futility and inescapable challenge, and the fact that these assays trigger behavioral state switching, motivated our consideration of the effects of ketamine on futility-induced passivity. The forced swim test and related assays in mice, although generally not considered a model for depression,[18] have been extensively used to assess behavioral phenotypes that are altered in animal models of depression[14] and their reversal by antidepressant compounds.

Previous studies in zebrafish showed that ketamine exerts acute anxiolytic effects[19] in adult and larval zebrafish,[6] and in juvenile zebrafish, it demonstrated that ketamine suppresses passivity following inescapable shocks through modulation of habenular and raphe activity.[2] However, the acute effects of ketamine[20] on neural activity in these behavioral studies were not considered, rendering unclear the mechanisms through which ketamine's long-lasting effects on brain activity occurs, which other futility-related behaviors may be affected, and through which pathways this occurs. Furthermore, the futility-induced passivity behavior we previously characterized proceeds through several medullary brain regions with limited overlap with the habenula (Hb) and raphe and critically involves astroglia, motivating an examination of ketamine's acute and persistent effects on both neurons and non-neuronal cells in our behavioral context.

Ketamine, in mammals, acutely enacts dissociative anesthesia, but following recovery and at lower doses, it drives a rapid and long-lasting effect on learned-helplessness behavior in rodents and elicits antidepressant effects in humans.[17,21] Ketamine has many molecular targets,[22–24] including the widely expressed NMDA receptor (NMDAR),[17,25] and because of this promiscuity, ketamine likely modulates activity in many brain regions[20,26–28] across both neurons and non-neuronal cell types.[29] Indeed, previous work has identified many candidate regions, including the prefrontal cortex,[30] Hb,[2,31–33] serotonergic raphe,[2] and dopaminergic system.[34–37] Here we sought to interrogate the mechanisms of ketamine's brain-wide effects by leveraging the unique accessibility of the larval zebrafish's entire brain to functional imaging and perturbation during behavior. Because of the broad range of possibilities of ketamine's action on circuits, previous work in culture and brain slices showing that ketamine can affect astroglia,[38–40] and astroglial involvement in behavioral state change,[9,41–48] we surveyed activity in both neuronal and non-neuronal glial populations.[49–52]

RESULTS

Ketamine induces long-term suppression of futility-induced passivity in larval zebrafish

We adapted a previously reported assay for futility-induced passivity in virtual reality environments in paralyzed, fictively behaving larval zebrafish[9] to assess this behavior in unparalyzed fish (Figure 1A). Fish were embedded in agarose such that their heads were immobilized and their tails free to move. Using custom-built behavior apparatuses, we monitored swimming while delivering drifting grating visual stimuli (STAR Methods). Trials consisted of three phases: "rest," "closed loop," and "open loop" (Figure 1B). During rest, gratings were stationary. During closed loop, gratings steadily drifted forward to induce swimming via the OMR.[10,53] If fish swam during closed loop, the forward-moving gratings slowed down and reversed direction to signal forward self-motion[10] through effective swims. By contrast, during open loop, gratings also drifted forward, but swimming did not affect grating movement and was thus futile. Open loop induced an initial period of higher-vigor swimming followed by transient cessation of swimming (passivity), a type of giving-up response to swimming being futile.[9]

We first tested the effect of ketamine, an NMDAR antagonist widely used as a rapid-acting dissociative anesthetic.[54] Previous studies have shown that at lower doses, and after the dissociative effects disappear, ketamine elicits persistent antidepressant action.[17,21] Fish were exposed to a transient dose of 200 μg/mL ketamine and then allowed to recover from acute anesthetic effects. We subjected these fish (and vehicle-treated clutch controls) to the futility-induced passivity assay (Figure 1C).

As a dissociative anesthetic, ketamine profoundly affects motor behavior on acute timescales. We used two independent analyses to control for whether ketamine had any lasting effects on baseline motor activity after washout. First, we analyzed closed-loop swimming post-recovery and found that both treated and control fish exhibited normal swimming during closed-loop periods (Figures 1D–1F, S1A, and S1B; Video S1). Second, freely swimming fish exhibited identical swim rates between treated and untreated groups (Figure S1C). Together, these data indicate that ketamine does not induce prolonged changes in basic locomotion in larval zebrafish.

We next analyzed ketamine's effects on futility-induced passivity in the open-loop period. During open loop, as expected, untreated control fish transitioned between periods of swimming, struggle characterized by larger, uncoordinated tail deflections (Figures 1D and S1D; Video S1), and passivity (Figure 1D). In ketamine-treated fish, the duration of passivity during open loop was decreased (Figures 1F and 1G; Video S2) in a

Please cite this article in press as: Duque et al., Ketamine induces plasticity in a norepinephrine-astroglial circuit to promote behavioral perseverance, Neuron (2024), https://doi.org/10.1016/j.neuron.2024.11.011

CellPress
OPEN ACCESS

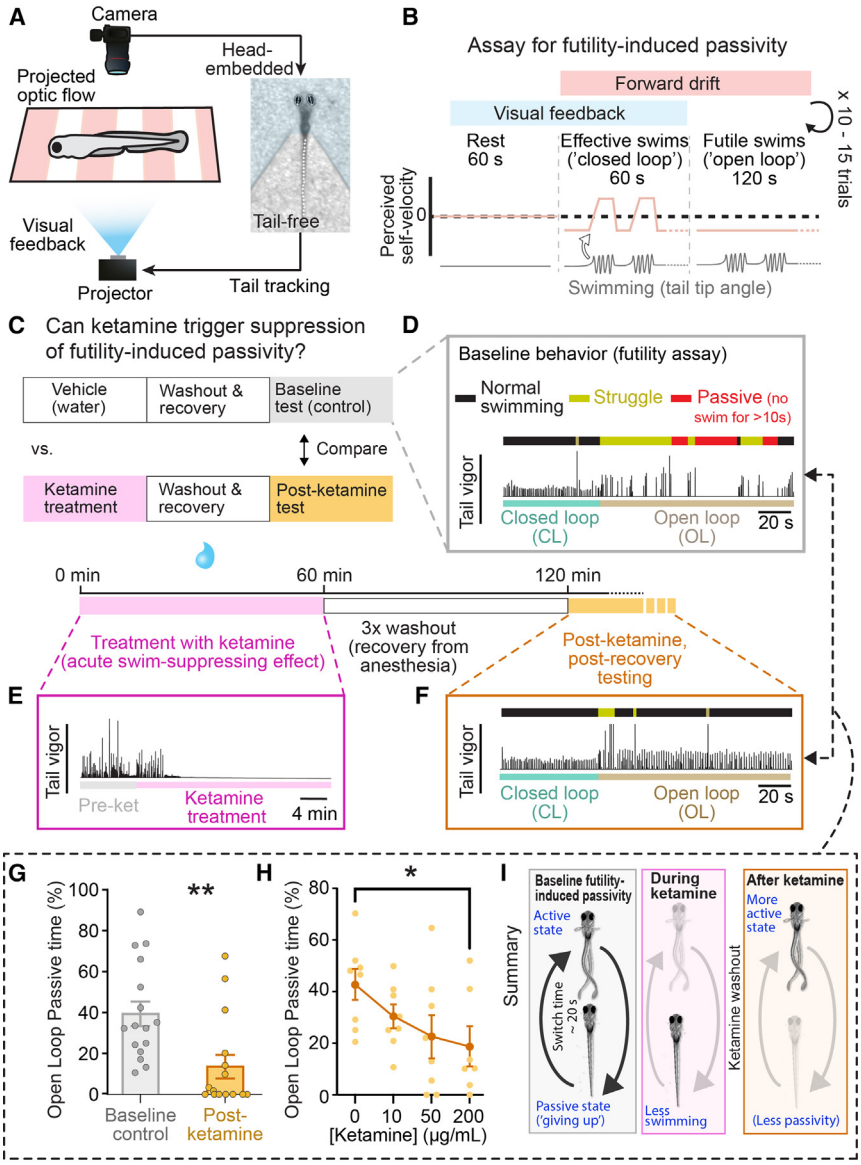

Figure 1. Brief ketamine exposure causes long-term suppression of futility-induced passivity in larval zebrafish

(A) Schematic of experimental workflow for imaging swimming behavior in unparalyzed larval zebrafish.

(B) Trial structure: 60 s of rest (no stimulus), 60 s of effective swimming ("closed loop," forward optic flow, visual feedback), then 120 s of futile swimming ("open loop," forward optic flow, no visual feedback), 10 to 15 repeated trials.

(C) Timeline of experiments testing ketamine's effect on futility-induced passivity.

(D) Example trials for vehicle control fish showing tail vigor (rolling-window tail angle standard deviation) across time. Colors above swim trace indicate normal swimming (black), struggle (yellow), and passivity (red). Colors below swim trace indicate closed- (teal) and open-loop (brown) periods.

(E) During ketamine treatment, fish tend to become quiescent.

(F) After ketamine treatment and washout, example fish swims similarly to vehicle-treated fish in closed loop (cf. D, CL period), but in open loop, they are less passive and more active.

(G) Ketamine-treated fish spend less time passive (periods > 10 s with no swimming) than vehicle controls during open loop. Mann-Whitney test, n = 16 fish (control), 15 fish (ketamine), $p = 0.0010$.

(H) Dose-response curve of ketamine's suppression of open-loop passive time. Mann-Whitney test, n = 8 fish (control), 8 fish (ketamine), $p = 0.0289$. All error bars denote standard error of the mean (SEM) * $p < 0.05$ ** $p < 0.01$.

(I) Summary of findings.

dose-dependent manner (Figure 1H). Post-ketamine, swim vigor in open loop was higher than in closed loop, showing that the decrease in passivity was not due to larvae failing to detect futile swims (Figure S1E). Nor was it due to slow motor recovery from anesthesia, as pre-exposure to the anesthetic sodium channel blocker MS-222 had no effect on futility-induced passivity (Figures S1F–S1H). Thus, ketamine suppresses futility-induced passivity and promotes behavioral perseverance in a manner distinct from its anesthetic or dissociative effects (Figure 1I).

Astrocytes exhibit similar calcium transients in fish and mice during futility-related behaviors

Futility-induced passivity in zebrafish shares features with learned-helplessness models such as the tail suspension test in rodents, which has been used for translational purposes to assess antidepressant action.[13] In both assays, attempts to leave an aversive situation are futile and include vigorous struggles and passivity. In zebrafish, futile locomotion elicits strong, often brain-wide calcium signaling in astrocytes[9] (Figures 2A–2C). To determine if astrocytes are similarly engaged during a learned-helplessness condition in mice, we monitored astrocyte calcium levels in the retrosplenial cortex (RSC), an accessible cortical region that receives dense noradrenergic innervation,[55,56] of *Aldh1l1-CreER;R26-lsl-GCaMP6s*[57] mice during the tail suspension test. For these studies, we employed a miniaturized, head-mounted two-photon microscope[58] that enabled stable visualization of GCaMP6s fluorescence within astrocytes through a chronic cranial window while mice were suspended (Figure 2D; Video S3). Periods of futile struggle in mice were associated with a gradual rise in astrocyte calcium levels throughout the imaging field, peaking at the transition from struggle to immobility, and returned to baseline levels as the mice ceased moving (Figures 2E, 2F, and S2A). These results indicate that the dynamics of astrocytic activity in mice are remarkably similar to those in zebrafish. Although the behaviors and brain regions are not identical, these results suggest that astrocyte engagement during intense arousal states is evolutionarily conserved, opening the possibility for cross-species comparisons of the effects of

Please cite this article in press as: Duque et al., Ketamine induces plasticity in a norepinephrine-astroglial circuit to promote behavioral perseverance, Neuron (2024), https://doi.org/10.1016/j.neuron.2024.11.011

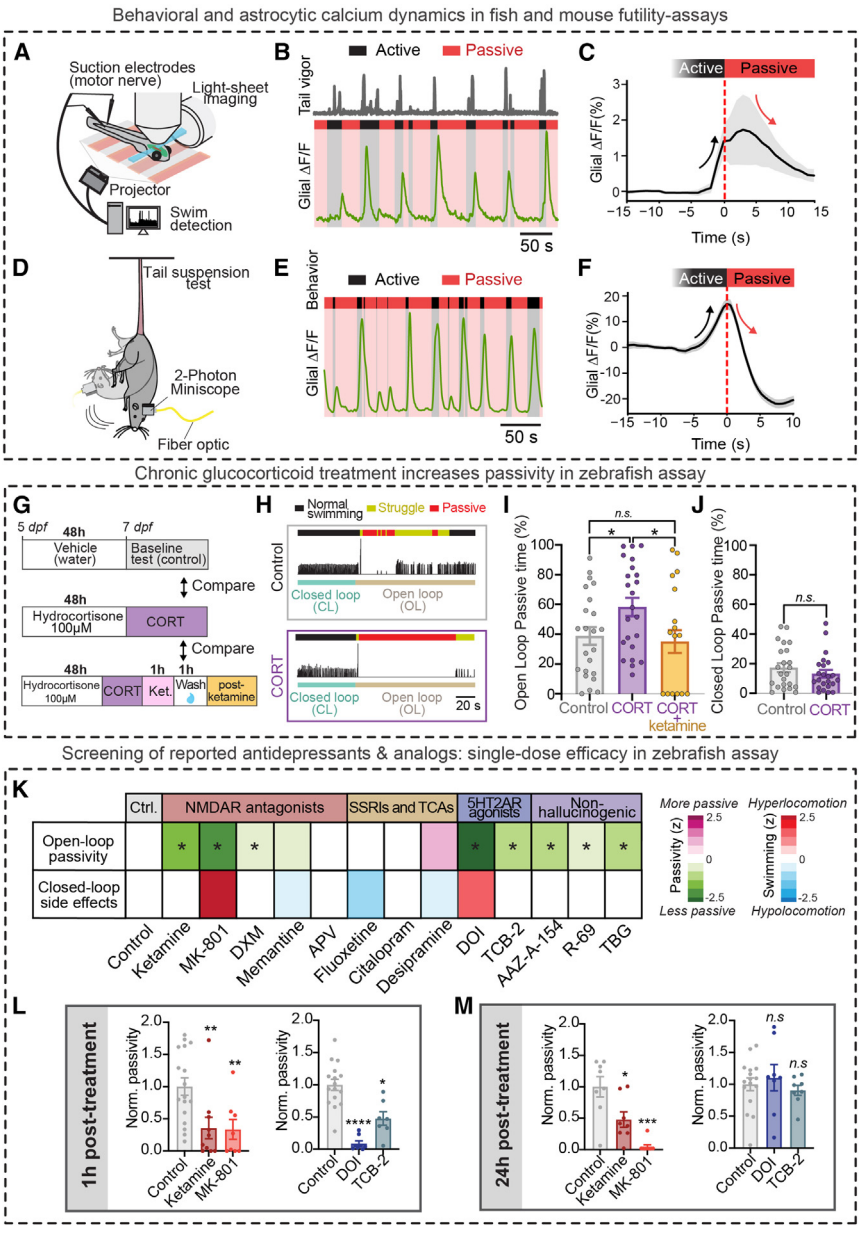

Figure 2. Translational potential and parallels between zebrafish and rodent futility-induced passivity assays

(A) A light-sheet microscope recorded from radial astrocytes across the brain at cellular resolution while fictive behavior was monitored, and visual stimulus was delivered.

(B) Swim traces (gray, tail vigor) showing active and passive periods and simultaneously recorded hindbrain astroglial calcium signals from an example fish.

(C) Average open-loop struggle-triggered jRGECO1a signal in hindbrain glia ($n = 3$).

(D) 2-photon imaging of cortical astrocyte calcium dynamics in the retrosplenial cortex using Aldh1l1-CreER and GCaMP6s mice using a head-mounted miniaturized microscope.

(E) Active and passive periods and simultaneously recorded cortical astrocyte calcium signals in the retrosplenial cortex from an example mouse.

(F) Average passivity-triggered cortical astrocytic signal. ($n = 8$).

(G) Timeline of experiments testing the effect of chronic hydrocortisone (CORT) treatment on futility-induced passivity in larval zebrafish.

(H) Example trials for control fish (K) and hydrocortisone-treated fish (L). Colors above swim trace indicate normal swimming (black), struggle (yellow), and passivity (red). Colors below swim trace indicate closed- (teal) and open-loop (brown) periods. Swim traces indicate tail vigor.

(I) CORT-treated fish spend more time passive than vehicle controls during open loop. This effect was reversed by treatment with ketamine. One-way ANOVA with Welch's correction for multiple comparisons, $n = 23$ (control), 23 (CORT), and 20 (ketamine-CORT). (CORT vs. control) $p = 0.0274$, (control vs. CORT-ketamine) $p = 0.7266$.

(J) Average percentage of closed-loop (CL) spent in the passive state. Mann-Whitney test, $n = 23$ (control), 23 (CORT), $p = 0.4453$.

(K) Open-loop passivity and closed-loop swim rate ("side-effects") of fish treated with vehicle (control) or various pharmacological compounds (normalized to mean of control) in the futility-induced passivity assay. Results are grouped by major pharmacological target of treatment compound. * Indicates $p < 0.05$ compared with control.

(L) Acute (1 h post-washout) effects of (left) phencyclidine-site NMDA receptor antagonists and (right) 5-HT2A receptor agonists on open-loop passivity.

(M) Persistent (24 h post-washout) effects of (left) phencyclidine-site NMDA receptor antagonists and (right) 5-HT2A receptor agonists. All error bars denote SEM. *n.s.* $p > 0.05$, * $p < 0.05$, ** $p < 0.01$, *** $p < 0.005$, **** $p < 0.001$. Statistics for (L) and (M) one-way ANOVA with Tukey's multiple comparison test (vs. control). (L, left), $n = 17$ (control), 10 (ketamine), 8 (MK-801), $p = 0.0086$ (ketamine), and 0.0115 (MK8-801). (L, right) 16 (control), 8 (DOI), 7 (TCB-2), $p = <0.0001$ (DOI), and 0.0008 (TCB-2). (M, left) $n = 8$ (control), 8 (ketamine), 8 (MK-801), $p = 0.0103$ (ketamine), <0.0001 (MK-801). (M, right) $n = 16$ (control), 8 (DOI), 8 (TCB-2), $p = 0.8096$ (DOI), and 0.8295 (TCB-2).

drugs on the neural pathways that control futility-related state-switching behavior.

Conserved pharmacologically induced behavioral state switching in fish and mice

The hypothesis that futility-induced passivity in zebrafish and rodent futility models engage similar cellular mechanisms would be bolstered if treatment with compounds known to increase or decrease passivity in futility-related assays exerted similar responses in these two species. Chronic glucocorticoid treatment[59] in mice is used as an animal model of depression, mimicking chronic hyperactivation of the HPA stress axis.[60] Among other behavioral phenotypes, such as decreased sucrose preference,[61] chronic glucocorticoid treatment induces increased passivity in the tail suspension test and forced swim test,[62,63] which can be reversed by treatment with

Please cite this article in press as: Duque et al., Ketamine induces plasticity in a norepinephrine-astroglial circuit to promote behavioral perseverance, Neuron (2024), https://doi.org/10.1016/j.neuron.2024.11.011

CellPress
OPEN ACCESS

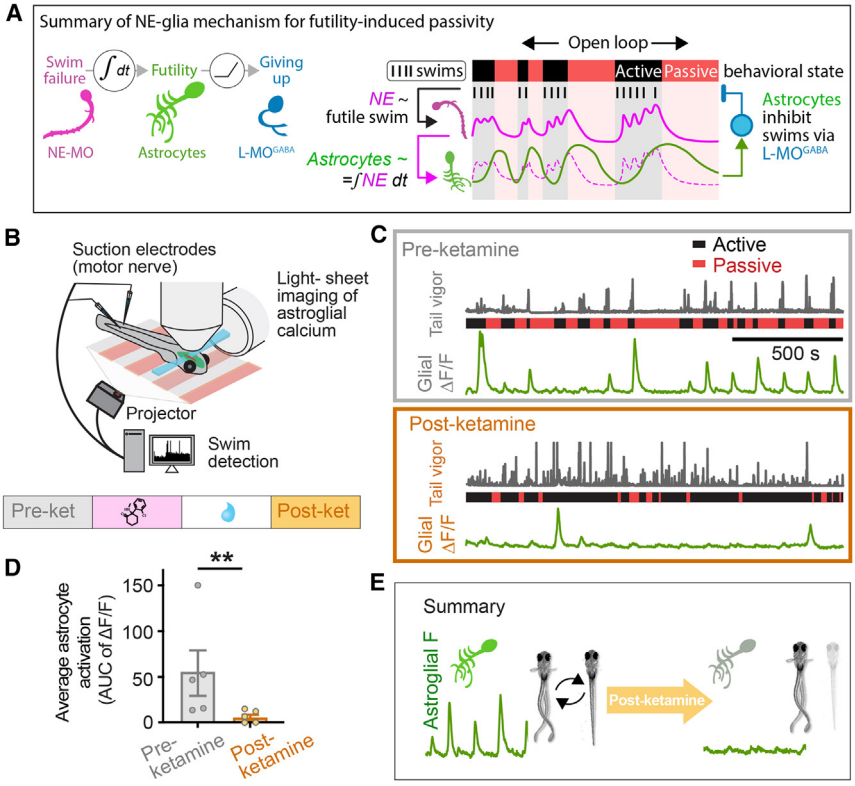

Figure 3. Brief ketamine exposure suppresses subsequent astrocyte calcium responses during futile swimming

(A) Summary of mechanism underlying futility-induced passivity in zebrafish, adapted from Mu et al.[9]

(B) Whole-brain imaging of radial astrocyte calcium during behavior as described in the main text.

(C) Swim traces (gray, tail vigor) showing active and passive periods and simultaneously recorded hindbrain astroglial calcium signals from two example *Tg(gfap:jRGECO1a)* fish either treated with vehicle control (pre-ketamine, top) or ketamine (post-ketamine, bottom). In both cases, fish were allowed to recover for 1 h following washout before recordings were performed.

(D) Astrocytes are less active in the open-loop test period after ketamine treatment compared with control, as assessed by comparing the average ΔF/F (area under the curve) of astrocytic calcium after strong-swims before and after ketamine treatment. Mann-Whitney test. $n = 5$ (pre), 6 (post). $p = 0.0087$.

(E) Summary of findings. Brief ketamine treatment causes, after washout, long-term reductions in passivity and hypo-activation of astrocytes compared with control.

antidepressants, including ketamine.[33] We found that long-term hydrocortisone pre-treatment (48 h) in larval zebrafish also increases futility-induced passivity (Figures 2G–2I), with open-loop-specific effects (Figure 2J), and that ketamine reversed this effect (Figure 2I). Thus, ketamine can reverse stress-hormone-induced changes in behavioral state switching in both mice and zebrafish.

In addition to ketamine, a broad range of compounds with known antidepressant effects in mammals produced similar outcomes in the zebrafish futility assay (Figures 2K–2M; Table S1). Compounds that have been previously reported to have fast-acting, antidepressant-like effects and that bind either NMDARs (ketamine, MK-801, DXM) (Figure 2L, left, and S2C) or serotonergic receptors (DOI) (Figure 2L, right) decreased futility-induced passivity, although MK-801 and DOI also induced hyperlocomotion during closed loop (Figure 2K). The 5-HT2A receptor agonist, TCB-2,[64] also suppressed futility-induced passivity (Figures 2K and 2L, right), similar to the effects of other psychedelics[65,66] in mammals. Finally, we tested recently synthesized psychedelic analogs with diverse chemical structures, including R-69, AAZ-A-154, and tabernanthalog (TBG).[67–69] We found that, as reported in rodent models, these compounds also significantly reduced passivity in zebrafish (Figures 2K, S2D, and S2E), demonstrating a conservation of their behavioral effects across species. Conversely, classical antidepressants that have prolonged onset times in rodents and humans,[70,71] such as selective serotonin reuptake inhibitors (SSRIs) and tryciclic antidepressants (TCAs), showed no passivity-suppressing effects after a single, 1-h dose in fish (Figure S2B). In addition, we examined the effects of two NMDAR antagonists, memantine and AP5, that do not affect passivity in mammals, and observed no significant effects on futility-induced passivity at the doses tested (Figures S2F and S2G).

A single dose of ketamine or psychedelics can produce behavioral effects that far outlast their presence in the body.[21,72–74] Consistent with these effects in mammals, both ketamine and MK-801 retained a passivity-suppressing effect 24 h after transient exposure (Figure 2M, left). Interestingly, normal passivity re-emerged 24 h after administration of the serotoninergic receptor agonists DOI and TCB-2 (Figure 2M, right). Therefore, ketamine triggers a persistent decrease in futility-induced passivity in larval zebrafish that reflects lasting alterations in brain activity. The similar pharmacological sensitivity between zebrafish and mouse futility behaviors suggests that it may be possible to exploit zebrafish as a more tractable model for interrogating circuit-level changes responsible for the effects of ketamine and other compounds on behavioral state transitions.

Brief ketamine exposure causes persistent changes in astroglial responsiveness to futility in fish

Previous studies in zebrafish indicate that the futility-induced switch to passivity is mediated by the noradrenergic-astroglial system.[9] Noradrenergic neurons in a brainstem cluster known as NE-MO,[9] likely corresponding to area A2 neurons in mammals,[75] activate during futility. Radial astrocytes integrate the noradrenergic futility signal and then activate neurons in the lateral medulla oblongata (L-MO^{GABA}) that suppress swimming (Figure 3A). To determine whether the decrease in passivity after ketamine exposure results from reduced astroglial activation, we

Please cite this article in press as: Duque et al., Ketamine induces plasticity in a norepinephrine-astroglial circuit to promote behavioral perseverance, Neuron (2024), https://doi.org/10.1016/j.neuron.2024.11.011

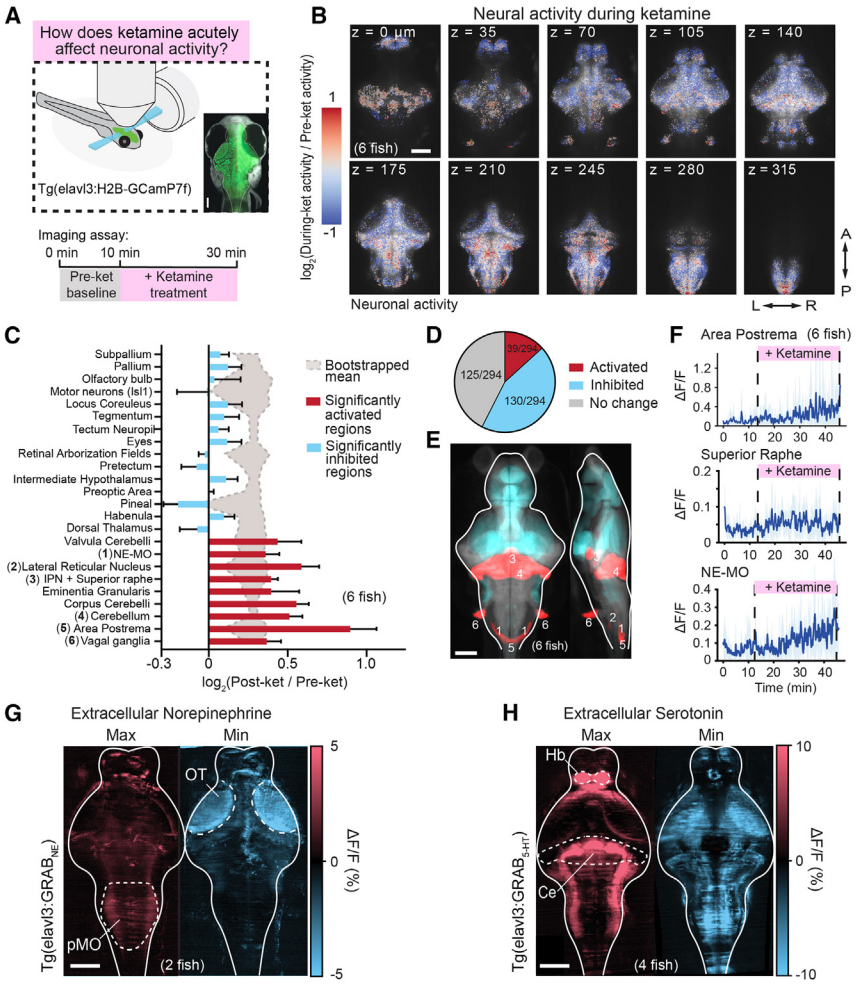

Figure 4. Activation of noradrenergic and serotoninergic populations following acute ketamine

(A) Fish expressing the nuclear calcium indicator H2B-GCaMP7f under a pan-neuronal promoter were imaged using a light-sheet microscope before and during acute treatment with ketamine. Micrograph shows orientation of larval zebrafish brain as shown in the following panels. Scale bar, 100 µm.

(B) Average activity changes across six registered fish (log-ratio of ΔF/F following ketamine administration to before administration) at different anatomical depths after ketamine treatment.

(C) Selected Z-Brain[76] areas activated significantly above (red) or below (blue) chance (background shaded region, 95% CI) following ketamine treatment. Chance levels determined through bootstrapping with shuffle indices (nBoot = 10,000). Numbers in parentheses correspond to regions in (E).

(D) Proportion of Z-Brain[76] areas activated significantly (same statistical assessment as in C) above, below, or at chance following ketamine treatment. A more comprehensive analysis for all areas is shown in Figure S4.

(E) Brain areas that were significantly (same statistical assessment as in C) activated or inhibited following ketamine treatment in blue or red overlaid onto the reference atlas fish. Labeled numbers correspond to regions listed in (C).

(F) Average neural activity (ΔF/F) of indicated noradrenergic and serotonergic regions across fish (n = 6 fish, top 10% cells for each region per fish). Shaded region denotes SEM.

(G) Maximum and minimum values (along the Z-dimension, top-bottom of the brain) for average NE levels across the brain during ketamine exposure imaged using $GRAB_{NE2h}$ (n = 2). OT, optic tectum, pMO, posterior medulla oblongata.

(H) Maximum and minimum values (along the Z-dimension, top-bottom of the brain) for average 5-HT levels across the brain during ketamine exposure imaged using $GRAB_{5\text{-}HT2.0}$ (n = 4). Ce, cerebellum, Hb, habenula. All scale bars, 100 µm.

measured astroglial calcium signals in *Tg(gfap:jRGECO1a)* fish during a fictive-swimming implementation of the futility assay (in which electrical signals in the tail are used in lieu of physical tail motion; Figure 3B). After ketamine exposure and washout, astroglial calcium levels were lower than untreated fish during futile swimming (Figures 3C–3E). This suggests that ketamine's effects on behavioral passivity may emerge from prolonged downregulation of astrocyte responsiveness to behavioral futility.

Acute brain-wide effects of ketamine on neural activity and neuromodulation

We used light-sheet imaging to collect activity profiles from single neurons across nearly the entire brain during acute ketamine exposure in *Tg(elavl3:H2B-GCaMP7f)* fish (Figure 4A). Images were then registered to a zebrafish brain atlas[76] to identify regions of concentrated activity (Figures S3A and S3B). Consistent with ketamine's inhibitory effects on spontaneous and sensory-evoked locomotion, neural activity was suppressed in early visual areas and hindbrain motor regions (Figures 4B–4D), with 130 out of 294 brain areas showing a significant reduction in activity (Figures 4D, S4B, and S4C). However, in a small subset of brain areas (39 out of 294 areas), neuronal activity was significantly enhanced by ketamine, including noradrenergic and serotonergic nuclei (Figures 4C–4E and S4A).

Due to the importance of monoaminergic systems on depressive phenotypes and their treatments, we examined ketamine's effects on the activity of noradrenergic and serotonergic nuclei in more detail. NE-MO neurons, along with other noradrenergic clusters in the area postrema, increased activity during ketamine exposure (Figures 4C–4F). In addition to the noradrenergic system, hindbrain serotonergic populations increased their activity during acute ketamine exposure (Figure 4F), consistent with observations in rodents.[77] To complement the assessment of neural activity changes in monoaminergic nuclei, we also directly visualized changes in both NE and 5-HT levels in the brain following ketamine treatment by imaging pan-neuronally expressed extracellular sensors of NE[78] (*Tg(elavl3:GRAB$_{NE2h}$)*)

Please cite this article in press as: Duque et al., Ketamine induces plasticity in a norepinephrine-astroglial circuit to promote behavioral perseverance, Neuron (2024), https://doi.org/10.1016/j.neuron.2024.11.011

CellPress
OPEN ACCESS

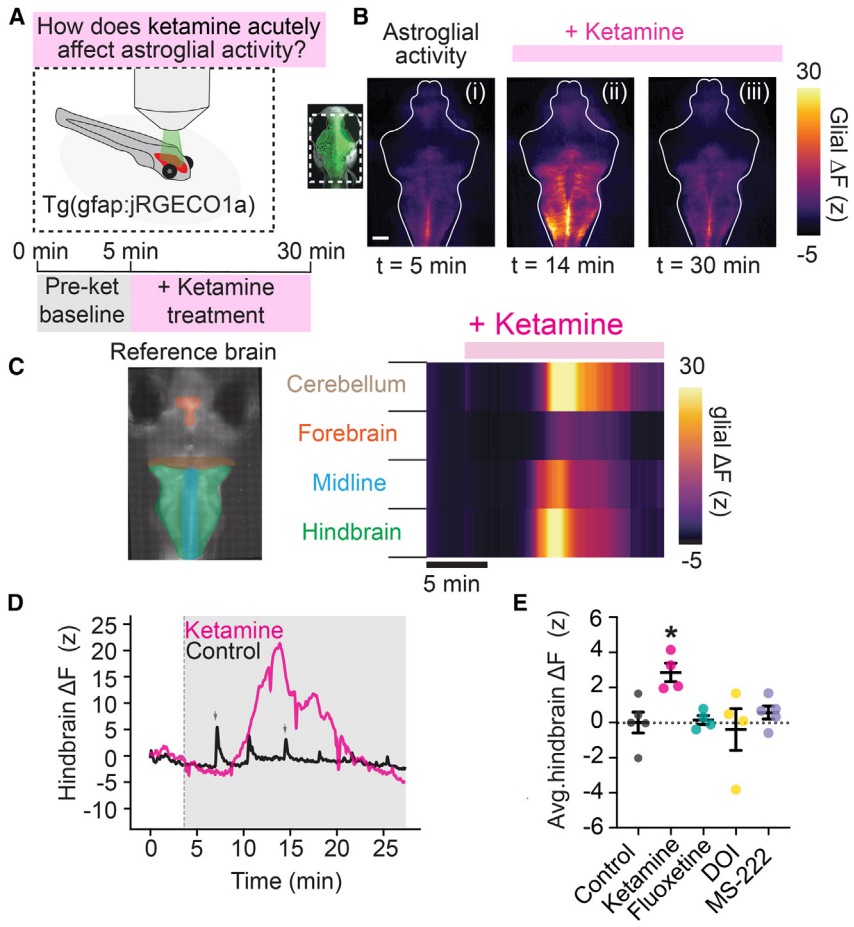

Figure 5. Ketamine triggers a long-lasting calcium elevation in astroglia

(A) Fish expressing the calcium indicator jRGECO1a in astroglia were imaged using an epifluorescence microscope before and during acute treatment with ketamine for 30 min.

(B) Example fluorescence micrographs of jRGECO1a signal at three time points illustrating elevation and return to baseline of cytosolic calcium in the presence of ketamine. Scale bar, 50 μm.

(C) Heatmap of glial jRGECO1a signal in four ROIs (left) for fish in (C). Pink bar indicates ketamine in the bath.

(D) Hindbrain jRGECO1a fluorescence change in an example fish treated with ketamine (200 μg/mL) or vehicle (control). Short increases in astrocytic calcium during struggles in control fish are indicated by gray arrowheads.

(E) Average hindbrain fluorescence change following treatment with listed compounds. Ketamine, but not fluoxetine (SSRI), DOI (5-HT2AR agonist), or MS-222 (anesthetic), elevates cytosolic astroglial calcium. One-way ANOVA with Tukey's multiple comparison test (vs. control). $n = 5$ (control, MS-222), 4 (all other conditions). $p = 0.0169$ (ketamine), 0.9395 (MS-222), 0.9893 (DOI), 0.9996 (fluoxetine).

(F) Summary of findings.

and 5-HT[79] (*Tg(elavl3:GRAB$_{5\text{-}HT2.0}$)*) (Figures S3C and S3D). We found that ketamine administration elevated NE across the hindbrain, especially in the posterior medulla oblongata (pMO), while NE levels decreased in the optic tectum (OT) (Figures 4G and S3E). Direct visualization of 5-HT revealed that ketamine-induced strong elevation in the Hb and cerebellum (Ce) but had more diverse effects in the OT and medulla (Figures 4H and S3F). Together, these data provide a brain-wide map of ketamine's effects on NE and 5-HT levels, indicating that ketamine acutely alters monoaminergic neuromodulation across the brain in a region-dependent manner.

NE-dependent elevation of astroglial calcium during acute ketamine exposure

NE is an evolutionarily conserved modulator of astroglial calcium signaling.[9,43,49–52,80] To determine if ketamine acts on NE modulation of astroglial calcium signaling, we imaged calcium activity in radial astrocytes during ketamine exposure using wide-field fluorescence imaging in unparalyzed, head-embedded *Tg(gfap:jRGECO1a)* fish (Figure 5A). Strikingly, acute exposure to ketamine induced a dose-dependent (Figures S5A–S5D) large rise in astroglial cytosolic calcium concentration (Figures 5B–5D; Video S4) that remained elevated for over 20 min (Figures S5F and S5G). This ketamine-induced calcium increase was many times larger and more prolonged than the transient calcium increases that occurred during open-loop struggles (magenta vs. black in Figure 5D). This effect was specific to ketamine, as it was not observed with fluoxetine, MS-222, or DOI (Figure 5E). These results raise the possibility that minutes-long activation of astroglia by NE during ketamine treatment plays a role in its suppression of future passivity behavior.

To determine whether the ketamine-induced astroglial calcium elevation depends on extracellular NE, we first performed simultaneous two-color brain-wide imaging of intracellular calcium in astroglia and extracellular NE (Figure 6A) in fish expressing jRGECO1a in astroglia and GRAB$_{NE2h}$ in neurons. NE elevation and astroglial calcium elevation had similar time courses (Figure 6B), and pharmacological inhibition of α1-adrenergic receptors (α1-ARs) (Figure 6C) with prazosin abolished the stimulatory effect of ketamine on astroglial calcium (Figure 6D). Moreover, pharmacological blockade of α1-AR signaling prevented the ability of ketamine to subsequently suppress futility-induced passivity (Figures 6E and S6A–S6C). Thus, ketamine triggers hyperactivation of astroglia through NE secretion and α1-AR activation. These data suggest that NE-dependent astroglial calcium hyperactivation is critical for reducing futility-induced passivity.

Please cite this article in press as: Duque et al., Ketamine induces plasticity in a norepinephrine-astroglial circuit to promote behavioral perseverance, Neuron (2024), https://doi.org/10.1016/j.neuron.2024.11.011

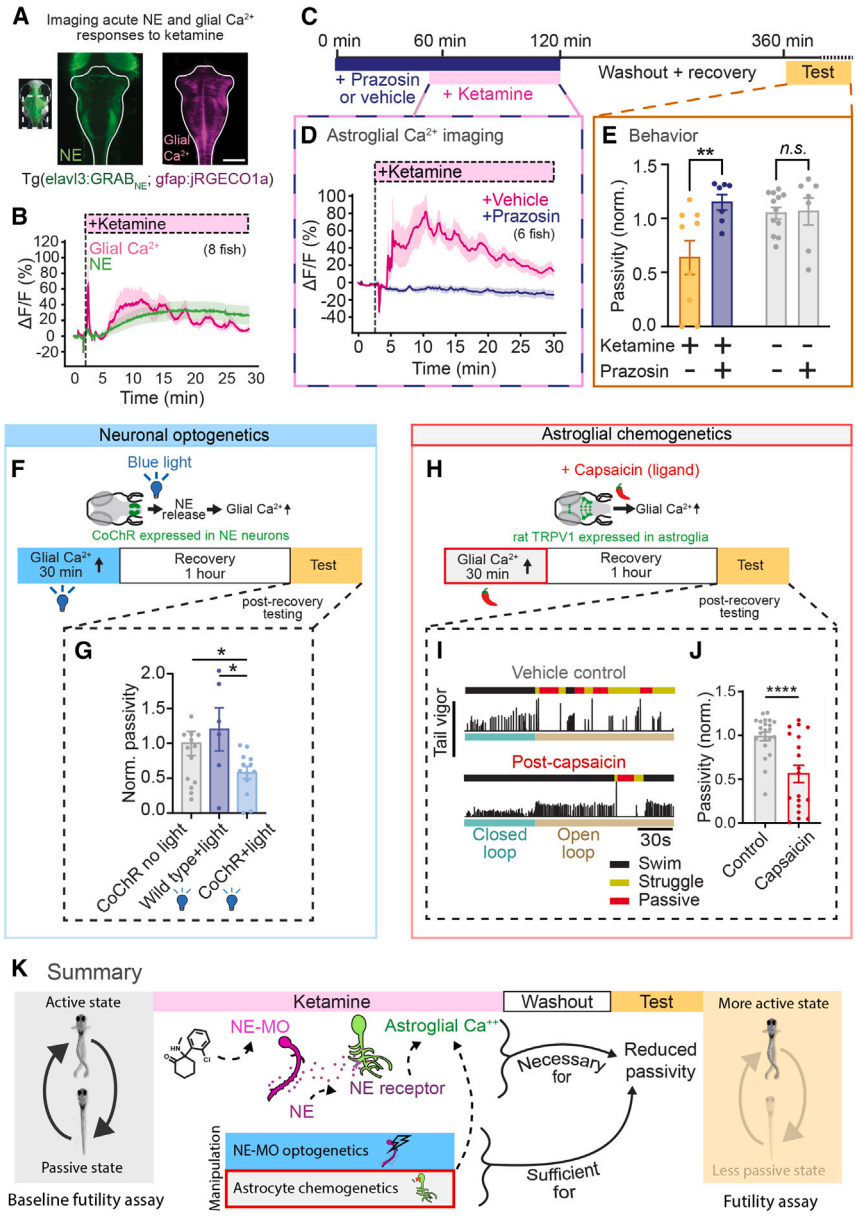

Figure 6. NE-dependent astroglial calcium elevation is required and sufficient for ketamine's behavioral effects

(A) Fluorescence image of a larval zebrafish expressing $GRAB_{NE2h}$ under the *elavl3* promoter (green) and jRGECO1a (glial Ca^{2+}) under the *gfap* promoter (pink). Scale bar, 100 μm.

(B) Simultaneously imaged intracellular glial Ca^{2+} dynamics (jRGECO1a signal) and extracellular NE dynamics ($GRAB_{NE2h}$ signal). Traces represent mean of fish (n = 8), and shaded regions denote SEM. Shaded region indicates ketamine (200 μg/mL) in bath.

(C) Schematic of experiments testing whether ketamine's effects on astroglial Ca^{2+} and futility-induced passivity behavior depend on NE signaling.

(D) Astroglial Ca^{2+} (jRGECO1a signal) response to ketamine (200 ug/mL) application in fish treated with 50 μM prazosin (n = 6) or vehicle control (n = 5).

(E) Open-loop passivity for fish treated with ketamine, with or without α1 adrenergic blocker prazosin (100 μM). All error bars denote SEM. * $p < 0.05$, ** $p < 0.01$, *n.s.* $p > 0.4$. ΔF (Z scored) for each fish was calculated as the difference between mean total fluorescence before treatment subtracted to total fluorescence at a specific time point, divided by the standard deviation of total fluorescence before treatment, for hindbrain mask (D). Two-way ANOVA with Sidak's multiple comparison test. n = 7 (control-prazosin and ketamine-prazosin), 9 (ketamine-vehicle), 11 (control-vehicle). p = Interaction (0.0140), 0.0057 (ket-prazosin vs. ket-vehicle), 0.9947 (control-vehicle. vs. control-prazosin).

(F) *Tg(dbh:KalTA4; UAS:CoChR-eGFP)* fish expressing the channelrhodopsin CoChR in norepinephrinergic (NE) neurons were continually stimulated optogenetically with blue (488 nm) light for 30 min. Fish were allowed to recover for an hour then assayed for futile swimming.

(G) Passivity normalized to clutch, non-stimulated controls. Optogenetic stimulation suppressed futility-induced passivity following recovery compared with non-stimulated clutch controls and non-expression controls stimulated with blue light. One-way ANOVA with Sidak's multiple comparison test. n = 19 (dbh:CoChr, no light), 14 (wild type, blue light), 13 (dbh:CoChr, blue). p = 0.0004 (WT-Blue light vs. DBH-Blue light), p = 0.0392 (WT-Blue light vs. DBH-no light), p = 0.0392 (DBH-no light vs. DBH-Blue light).

(H) Transgenic fish expressing rat TRPV1 in astroglia were treated with capsaicin for 30 min. After 30 min, capsaicin was washed out and fish allowed to recover for 1 h before being tested.

(I) Example swimming of capsaicin-treated fish (bottom) and untreated clutch controls (top). Black, yellow, and red segments above swim vigor trace denote regular swimming, struggling, and passivity, respectively.

(J) Passivity normalized to untreated clutch controls. Capsaicin-treated fish exhibit decreased futility-induced passivity, although the distribution of passivity duration is bimodal. Mann-Whitney test. n = 22 (control), 19 (capsaicin), p = 0.0005.

(K) Summary of findings.

Transient opto/chemogenetic astroglial calcium elevation causes long-term suppression of futility-induced passivity

To assess whether the aftereffects of elevated astrocytic calcium are sufficient to suppress passivity, we induced transient (~30 min) calcium elevations in astroglia using two different methods and assayed futility-induced behavior afterward. First, we optogenetically activated noradrenergic neurons in *Tg(dbh:KalTA4; UAS:CoChR-eGFP)* fish,[9] which express the channelrhodopsin CoChR[81] (Figure 6F) in noradrenergic

Please cite this article in press as: Duque et al., Ketamine induces plasticity in a norepinephrine-astroglial circuit to promote behavioral perseverance, Neuron (2024), https://doi.org/10.1016/j.neuron.2024.11.011

CellPress
OPEN ACCESS

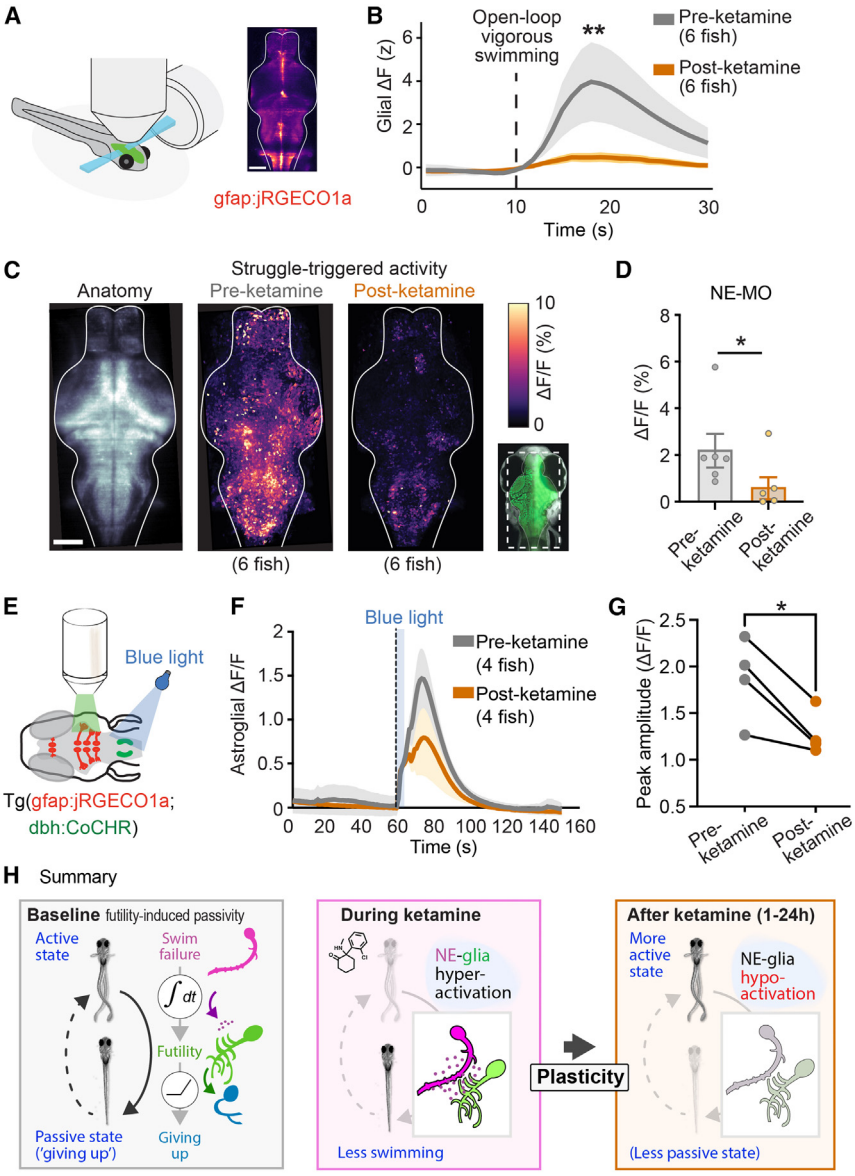

Figure 7. Persistent suppression of futility-activated neuron-astroglial circuits following ketamine exposure

(A) A light-sheet microscope recorded from most radial astrocytes and neurons in the brain at cellular resolution (STAR Methods).

(B) Astrocyte jRGECO1a signal following standardized strong swims in fish before and treatment with ketamine Same dataset as Figure 3D. Mann-Whitney test. $n = 5$ (pre), 6 (post). $p = 0.0087$.

(C) Left: anatomical max projection of *Tg(elavl3:H2B-GCaMP7f)* fish imaged during behavior. (middle) max projection of futile-swim-triggered neural activity of untreated fish ($n = 6$). Right: max projection of futile-swim-triggered neural activity of ketamine-treated fish shown pre-ketamine and post-ketamine ($n = 6$).

(D) Average struggle-triggered ΔF/F in NE-MO cells before and after ketamine treatment. Mann-Whitney test. $n = 6$ (pre), 6 (post). $p = 0.041$.

(E) Transgenic fish expressing the channelrhodopsin CoChR in norepinephrinergic (NE) neurons and the calcium sensor jRGECO1a in glia were briefly stimulated optogenetically with blue (488 nm) light for 5 s while recording glial activity.

(F) Average ΔF/F traces showing glial calcium responses after NE-MO stimulation with blue light, before (pre-ket) and after (post-ket) ketamine treatment, with different fish for pre/post.

(G) Peak amplitude (ΔF/F) following blue light stimulation in the same pre-ket and post-ket fish. Two-tailed paired t test. $n = 4$ pairs. $p = 0.0268$. All error bars denote SEM. * $p < 0.05$, ** $p < 0.01$.

(H) Summary of findings.

neurons. Continuous optogenetic activation of NE neurons with blue light (488 nm) for 30 min induced a minutes-long calcium rise in hindbrain radial astroglia similar to that induced by ketamine, albeit with a faster decay rate (Figures S6D–S6G). This optogenetic NE neuron activation led to decreased futility-induced passivity 1 h later (Figure 6G), indicating that the aftereffects of strong, transient NE-MO activation and associated astroglial calcium elevation are sufficient to mimic ketamine's lasting effects on behavior.

Second, we selectively activated astroglia by chemogenetically stimulating astroglia that express the rat transient receptor potential V1 channel (TRPV1) (Figures 6H and S5H; STAR Methods). Native TRPV1 in zebrafish is not sensitive to the chemical capsaicin, but rat TRPV1 is activated by capsaicin and induces calcium influx.[9,82] In TRPV1-expressing fish, capsaicin reliably led to stronger and longer-lasting astroglial calcium events (Figure S6I) compared with futility-induced passivity events and caused a long-term suppression of futility-induced passivity after washout (Figures 6I and 6J). Capsaicin did not affect wild-type fish (Figure S6L). Pharmacological inhibition of α1-AR had no effect on capsaicin-induced suppression of passivity (Figures S6J and S6K), consistent with the behavioral effects of astroglial hyperactivation being downstream of NE and α1-AR (Figure 6K). Thus, prolonged and strong calcium increases in astrocytes are sufficient to downregulate future futility-induced passivity.

Brief exposure to ketamine causes long-term suppression of neuronal and astroglial responses to futility

One explanation for how transient hyperactivation of astrocytes by ketamine leads to long-term passivity suppression is that astroglia and potentially neurons become less responsive to futile swims after ketamine exposure. To identify brain regions with long-lasting activity changes, we performed near-whole-brain light-sheet imaging of neuronal and astroglial calcium activity in *Tg(elavl3:H2B-jGCaMP7f; gfap:jRGECO1a)* fish after recovery from exposure to ketamine. We first assessed the

Please cite this article in press as: Duque et al., Ketamine induces plasticity in a norepinephrine-astroglial circuit to promote behavioral perseverance, Neuron (2024), https://doi.org/10.1016/j.neuron.2024.11.011

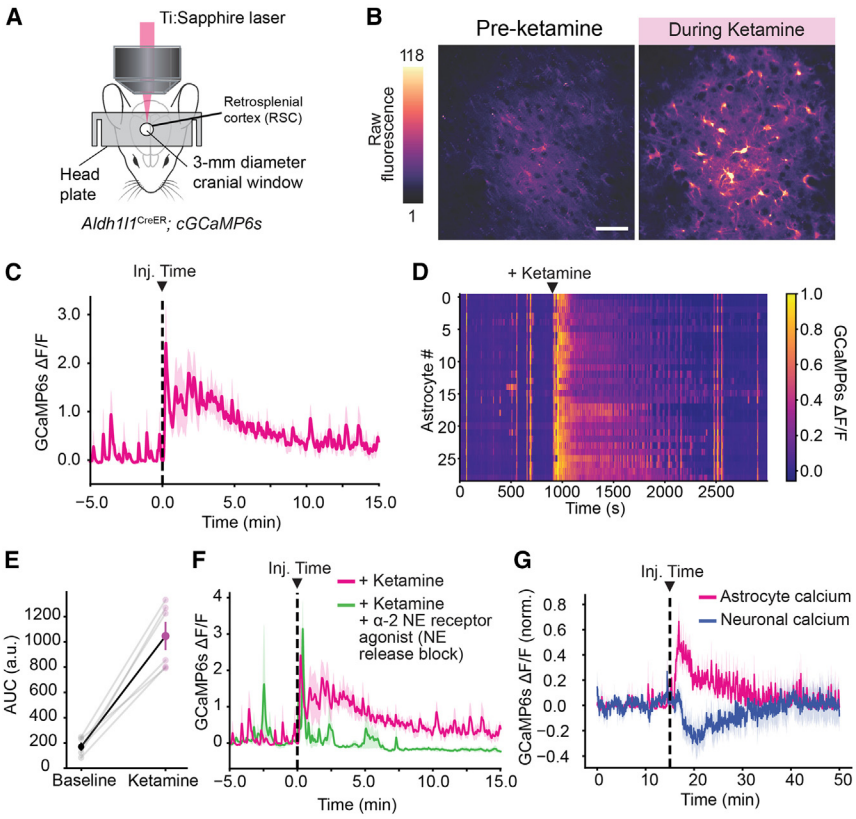

Figure 8. Ketamine elevates astrocytic calcium in mammalian astrocytes *in vivo* through conserved signaling pathways

(A) Schematic showing setup for *in vivo* imaging of cortical astrocytic calcium in awake mice.

(B) Fluorescence micrographs of GCaMP6s signal in the retrosplenial cortex (RSC), for an example mouse at two time points illustrating elevation of cytosolic calcium following IP injection of 20 mg/kg ketamine. Scale bar, 50 μm.

(C) Average RSC ΔF/F trace in response to 20 mg/kg ketamine (n = 6), injected at 15 min (dotted line).

(D) ΔF/F for individual astrocytes over time in response to 20 mg/kg ketamine (black arrow).

(E) Quantification of RSC fluorescence change before and after ketamine injection, normalized to control. Paired two-tailed test. n = 6. p = 0.0003.

(F) Average RSC ΔF/F trace for mice injected with 20 mg/kg ketamine or 20 mg/kg ketamine plus 0.05 mg/kg of an alpha-2 agonist, dexmedetomidine. n = 5. ** $p < 0.01$.

(G) Average RSC ΔF/F trace for astrocytes (pink) and excitatory neurons (blue) in response to 20 mg/kg ketamine, injected at 15 min (dotted line) using Aldh1l1-CreER;GCaMP6s;Thy1-jRGECO mice. n = 4.

responsiveness of hindbrain astroglia to open-loop swimming.[9] To control for differences in swim vigor, which might affect neural and astroglial responses, we analyzed swim-triggered responses in only high-vigor, struggle-like swims during open loop (Figures S7E and S7F). This revealed that, while the struggles had similar vigors pre- and post-ketamine treatment (Figure S7G), astroglial calcium responses to futile swims were markedly diminished in ketamine-treated fish relative to controls (Figures 7A and 7B, consistent with Figures 3C–3E), an effect that was not observed in vehicle-treated controls (Figures S7A–S7D). Because surges in astroglial calcium are known to trigger the passive behavioral state in futility-induced passivity,[9] this decrease in the glial calcium response to futile swims provides a possible explanation for the decline in futility-induced passivity.

A decrease in astroglial response to futility could arise from weaker noradrenergic modulation or from an astroglial-autonomous decline in sensitivity to NE. To investigate the contribution of decreased futility-triggered neural activity, we analyzed brain-wide neural activity and astroglial calcium signals during the trials shown in Figures 7B, S7E, and S7F. There was a significant decrease in futile struggle-triggered neural responses across the brain, including in NE-MO (Figures 7C and 7D). To determine if ketamine reduces the sensitivity of astroglia independent of changes in NE neuron activity, we assessed their response to strong, selective, optogenetic activation of noradrenergic neurons (Figure 7E). Astroglial calcium responses to this mode of NE neuron stimulation were suppressed for at least 1 h after ketamine washout (Figures 7F and 7G). These results, together with the pharmacological silencing and chemo/optogenetic activation (Figure 6) results, show that brief ketamine exposure results in lasting desensitization of the NE-astroglial circuit (Figure 7H).

Ketamine induces an acute increase in astrocyte calcium activity in mice

NE and related molecules directly increase astroglial calcium in flies, fish, and mammals,[43,49–52,80] indicating high evolutionary conservation of this modulatory pathway. Ketamine enhances NE release in the mammalian brain,[27] suggesting that mammalian astrocyte activity may be enhanced by ketamine. However, a previous study showed that the ketamine/xylazine combination used routinely for anesthesia in mice suppresses astrocytic calcium levels.[83] Because xylazine is known to suppress noradrenergic signaling through its activation of auto-inhibitory α2 ARs, we re-examined the effect of ketamine on mammalian astrocytes in unanesthetized animals. We monitored astrocyte calcium levels in *Aldh1l1-CreER;R26-lsl-GCAMP6s* mice using a two-photon microscopy in head-fixed, awake animals (Figures 8A and S8A). As in Figures 2D–2F, we imaged astrocytes from the RSC, a region implicated in producing the dissociative effects of ketamine.[84] Acute intraperitoneal injection of ketamine induced a striking, widespread increase in astrocytic calcium (Figure 8B; Video S5). The calcium response to ketamine peaked several minutes after injection and lasted for >10 min in all animals tested (Figures 8C–8E and S8F–S8I), similar to the time course seen in zebrafish. By contrast, mice injected with vehicle alone exhibited only a brief, short latency calcium rise (Figures S8B–S8E), presumably due to the arousing effects of the injection. The astrocyte

Please cite this article in press as: Duque et al., Ketamine induces plasticity in a norepinephrine-astroglial circuit to promote behavioral perseverance, Neuron (2024), https://doi.org/10.1016/j.neuron.2024.11.011

calcium elevation within the field of view consisted of both a plateau response that slowly waned and an increase in discrete calcium transients (Figures S8F–S8I). These responses were abolished by treatment with dexmedetomidine (0.01 mg/kg), an inhibitor of NE release (Figure 8F). To assess the relationship between this astrocyte calcium rise and the activity of surrounding neurons, we simultaneously imaged astrocyte and neuronal calcium levels in *Aldh1l1-CreER;GCaMP6s;Thy1-jRGECO* mice, which express GCaMP6s in astrocytes and jRGECO in excitatory neurons (Figure 8G). Similar to our observations in larval zebrafish, ketamine injection led to decreased neuronal activity that mirrored the increased glial calcium. Although the brain regions are different, these data indicate that on the cell-type and neuromodulator level, ketamine engages an evolutionarily conserved mode of astrocyte neuromodulation to alter the behavioral response to futility.

DISCUSSION

Here we showed that a single dose of ketamine causes a persistent increase in behavioral perseverance primarily by inducing plasticity within a hindbrain neuromodulatory circuit consisting of astroglia and neurons. Ketamine acutely triggers a hyper-noradrenergic brain state that causes prolonged astroglial calcium elevation. Following washout and return of astroglial calcium to baseline, desensitization occurs within the hindbrain futility circuit. As a result, this noradrenergic-astroglial circuit becomes less sensitive to futility, leading to persistent behavioral changes, specifically, increased behavioral perseverance.

The primary implication of these studies is that the long-lasting behavioral effects of ketamine, including its rapid and persistent antidepressant effects, should be re-evaluated in the context of its rapid, profound effects on endogenous monoaminergic neuromodulation and neuron-astroglial communication. Dysfunction in monoaminergic signaling has long been linked to depression in patients and animal models of depression,[85] and conventional antidepressant treatments affect monoamine levels by inhibiting their reuptake. Our work supports a mechanism in which ketamine not only targets monoaminergic neuromodulatory systems but also exerts its long-term behavioral effects through a process involving astrocytes. Unlike monoamine reuptake inhibitors, ketamine acts as an impulse perturbation, where a transient but rapid and profound monoaminergic elevation leads to long-lasting effects. These dynamics suggest an acute dose of ketamine engages endogenous homeostatic mechanisms to persistently alter monoaminergic neuromodulation. Intriguingly, the critical role of rapid NE elevation and astroglial α1-AR activation in persistent resilience may explain several alternative antidepressant interventions in rodent models and patients, such as transcranial direct current stimulation (tDCS) and vagal nerve stimulation (VNS). tDCS activates astrocytes in rodents,[86] suggesting the antidepressant effects of tDCS invoke similar molecular components (NE and astrocyte α1-ARs) as the futility pathway in larval zebrafish.[9] VNS has antidepressant effects in patients[87] and rodent models.[88] Intriguingly, the vagus nerve may provide input to NE-MO and homologous mammalian regions,[75] and thus VNS may act as an NE impulse perturbation similar to ketamine. Thus, our study raises the possibility that diverse treatments converge onto a common hindbrain NE-astroglial network to induce rapid and sustained antidepressant effects.

Emerging evidence demonstrates that astroglia play important and evolutionarily conserved roles in brain state modulation.[41,43,49,50,80,89] Our work suggests potential links between astroglial modulation of brain state with previous work on the role of astroglia in both depression and the efficacy of antidepressants. Astrocytes respond to NE[9,49–52] and serotonin[48] with elevations in cytosolic calcium. Furthermore, astroglial responsiveness to neuromodulators, such as norepinephrine in the Hb[90] or serotonin in the medial prefrontal cortex (mPFC),[48] has recently been shown to be disrupted in rodent depression models, and stimulating mPFC astrocytes chemogenetically rescues depression-related behavioral phenotypes.[48] Our results provide *in vivo* evidence in behaving animals that ketamine-evoked enhancement of monoaminergic signaling to astrocytes plays a key role in suppressing futility-induced passivity after washout. The ability to monitor astrocyte calcium dynamics in freely moving mice with miniature 2P microscopes and multi-core fiber optic systems may reveal distinct features of astrocyte network activity associated with different behaviors. The calcium dynamics within astrocytes during the tail suspension test and ketamine exposure were remarkably similar to astroglial responses in zebrafish. We note that the region recorded in mice is different from the regions that play a central role in zebrafish—such as L-MO[9]—because the analogous region in mice is still unknown. For this reason, we chose a region in the mouse that is easily accessible for imaging and receives dense noradrenergic innervation. Together, in terms of behavior, cell types, and neuromodulators involved, we reasoned that these systems are sufficiently analogous to investigate potential commonalities. During movement in futile environments—tail suspension in mice, open-loop optic flow in fish—astrocyte calcium rose and peaked near the time of the behavioral transition to passivity. In both animals, ketamine elicited a prolonged rise in astrocyte calcium, which depended on NE. These commonalities open the possibility that further mechanistic studies in zebrafish may help understand key steps in this process that could ultimately be targeted for therapeutic development. However, further studies considering astrocytic calcium activity in other relevant regions such as the mPFC[30,48] or the Hb[25,32] will provide important complementary insights into ketamine's action on glia and behavioral transitions in mammals.

We found that even transient astroglial activation has profound, lasting effects on neural circuit activity and animal behavior. The reduction in sensitivity of NE-MO neurons and astroglia may represent homeostatic responses to extreme hyperactivation during ketamine presence. Previous studies demonstrated that prolonged exposure to NE can lead to receptor desensitization.[91] It is also possible that the calcium elevation in astrocytes causes long-lasting changes in other astroglial physiological properties, such as expression of Kir4.1.[32,92] Our studies suggest that the potent effects of ketamine may reflect a previously unrecognized synergy between NE modulation of astrocyte calcium and direct NMDAR inhibition[31] on neurons as a means to pharmacologically reduce futility-induced state switching. Understanding how fast-acting antidepressants act

on non-neuronal cell types to alter their interaction with key behavioral circuits could lead to new insight into the cellular and circuit pathways that go awry during major depressive disorder and provide the means to design new fast-acting, effective therapeutics.[6,93]

RESOURCE AVAILABILITY

Lead contact

Further information and requests for resources should be directed to and will be fulfilled by the lead contact, Misha B. Ahrens (ahrensm@janelia.hhmi.org).

Materials availability

All fish lines generated in this study are available from the lead contact without restriction.

Data and code availability

All plots were generated using Prism (GraphPad) or Python, and Prism files used to generate plots have been deposited on GitHub (10.5281/zenodo.14174436) along with Jupyter notebooks (Python 3.7) used to process raw data. Additional raw data and Python and C++ code used are available from the lead contact upon request.

ACKNOWLEDGMENTS

This research was supported by the Boehringer Ingelheim Fonds Graduate Fellowship to M.D. and A.R.; German Research Foundation SPP1757 SA2114/2 to G.S.; Howard Hughes Medical Institute to A.B.C., M.D., S.N., and M.B.A.; NIH grant 1R01NS126043 to A.E.C. and S.B.; NIH grant P30 NS050274 and P50 MH084020 to D.E.B.; NIH grant 1R01GM128997 to D.E.O.; NIH grant R35 NS122172 to D.A.P.; NIH grant U19NS104653, 1R01NS124017, and IIS-1912293 to F.E.; NSF GRFP DGE1745303 to A.B.C.; NSF GRFP DGE2139757 to E.H. and Simons Foundation SCGB 542943SPI to F.E. and M.B.A. We thank the Harvard Center for Biological Imaging (RRID:SCR_018673) for infrastructure and support. We would like to thank Dr. Bryan Roth, Dr. Jon Ellman, and their labs for providing us with R-69. We would like to thank the Janelia Visiting Scientist Program for support. We would like to thank all laboratory members for feedback, Mark Ellisman for discussions, and Brett Mensh, Andrew Bolton, Kristian Herrera, Vickie Wang, Takashi Kawashima, Michael Yartsev, and Yu Mu for advice on the manuscript. We would like to thank Herriet Hsieh for discussions and comments on the manuscript and Sabrina Boutselis for designing the red hot chili pepper illustration.

AUTHOR CONTRIBUTIONS

Conceptualization, M.D., A.B.C., M.C.F., and M.B.A.; methodology, M.D., A.B.C., E.H., S.N., S.B., G.S., A.R., and D.A.P.; investigation, M.D., A.B.C., and E.H.; visualization, M.D., A.B.C., and E.H.; writing – original draft, M.D. and A.B.C.; writing – review & editing, M.D., A.B.C., E.H., A.E.C., D.E.O., D.E.B., M.C.F., F.E., and M.B.A.; funding acquisition, A.E.C., D.E.O., D.A.P., D.E.B., M.C.F., F.E., and M.B.A.; project administration, M.C.F., F.E., and M.B.A.; supervision, A.E.C., D.E.O., D.E.B., M.C.F., F.E., and M.B.A.

DECLARATION OF INTERESTS

D.E.O. is a co-founder of Delix Therapeutics, Inc., serves as the Chief Innovation Officer and Head of the Scientific Advisory Board, and has sponsored research agreements with Delix Therapeutics. Delix Therapeutics has licensed technology from the University of California, Davis. A.E.C. is a co-founder of Q-State Biosciences.

STAR★METHODS

Detailed methods are provided in the online version of this paper and include the following:

SUPPLEMENTAL INFORMATION

Supplemental information can be found online at https://doi.org/10.1016/j.neuron.2024.11.011.

Received: March 16, 2024
Revised: August 8, 2024
Accepted: November 20, 2024
Published: December 17, 2024

REFERENCES

1. Flavell, S.W., Gogolla, N., Lovett-Barron, M., and Zelikowsky, M. (2022). The emergence and influence of internal states. Neuron *110*, 2545–2570.
2. Andalman, A.S., Burns, V.M., Lovett-Barron, M., Broxton, M., Poole, B., Yang, S.J., Grosenick, L., Lerner, T.N., Chen, R., Benster, T., et al. (2019). Neuronal Dynamics Regulating Brain and Behavioral State Transitions. Cell *177*, 970–985.e20.
3. Bhandiwad, A.A., Chu, N.C., Semenova, S.A., Holmes, G.A., and Burgess, H.A. (2022). A cerebellar-prepontine circuit for tonic immobility triggered by an inescapable threat. Sci. Adv. *8*, eabo0549.
4. Swaminathan, A., Gliksberg, M., Anbalagan, S., Wigoda, N., and Levkowitz, G. (2023). Stress resilience is established during development and is regulated by complement factors. Cell Rep. *42*, 111973.
5. Lovett-Barron, M., Andalman, A.S., Allen, W.E., Vesuna, S., Kauvar, I., Burns, V.M., and Deisseroth, K. (2017). Ancestral Circuits for the Coordinated Modulation of Brain State. Cell *171*, 1411–1423.e17.
6. Braun, D., Rosenberg, A.M., Rabaniam, E., Haruvi, R., Malamud, D., Barbara, R., Aiznkot, T., Levavi-Sivan, B., and Kawashima, T. (2024). High-resolution tracking of unconfined zebrafish behavior reveals stimulatory and anxiolytic effects of psilocybin. Mol. Psychiatry *29*, 1046–1062. https://doi.org/10.1038/s41380-023-02391-7.
7. Langebeck-Jensen, K., Shahar, O.D., Schuman, E.M., Langer, J.D., and Ryu, S. (2019). Larval Zebrafish Proteome Regulation in Response to an Environmental Challenge. Proteomics *19*, e1900028.
8. Chen, J., Poskanzer, K.E., Freeman, M.R., and Monk, K.R. (2020). Live-imaging of astrocyte morphogenesis and function in zebrafish neural circuits. Nat. Neurosci. *23*, 1297–1306.

9. Mu, Y., Bennett, D.V., Rubinov, M., Narayan, S., Yang, C.-T., Tanimoto, M., Mensh, B.D., Looger, L.L., and Ahrens, M.B. (2019). Glia Accumulate Evidence that Actions Are Futile and Suppress Unsuccessful Behavior. Cell *178*, 27–43.e19.
10. Orger, M.B., Smear, M.C., Anstis, S.M., and Baier, H. (2000). Perception of Fourier and non-Fourier motion by larval zebrafish. Nat. Neurosci. *3*, 1128–1133.
11. Naumann, E.A., Fitzgerald, J.E., Dunn, T.W., Rihel, J., Sompolinsky, H., and Engert, F. (2016). From Whole-Brain Data to Functional Circuit Models: The Zebrafish Optomotor Response. Cell *167*, 947–960.e20.
12. Kawashima, T., Zwart, M.F., Yang, C.-T., Mensh, B.D., and Ahrens, M.B. (2016). The Serotonergic System Tracks the Outcomes of Actions to Mediate Short-Term Motor Learning. Cell *167*, 933–946.e20.
13. Cryan, J.F., Mombereau, C., and Vassout, A. (2005). The tail suspension test as a model for assessing antidepressant activity: review of pharmacological and genetic studies in mice. Neurosci. Biobehav. Rev. *29*, 571–625. https://doi.org/10.1016/j.neubiorev.2005.03.009.
14. Unal, G., and Canbeyli, R. (2019). Psychomotor retardation in depression: A critical measure of the forced swim test. Behav. Brain Res. *372*, 112047. https://doi.org/10.1016/j.bbr.2019.112047.
15. Seligman, M.E., and Beagley, G. (1975). Learned helplessness in the rat. J. Comp. Physiol. Psychol. *88*, 534–541. https://doi.org/10.1037/h0076430.
16. Porsolt, R.D., Le Pichon, M., and Jalfre, M. (1977). Depression: a new animal model sensitive to antidepressant treatments. Nature *266*, 730–732.
17. Autry, A.E., Adachi, M., Nosyreva, E., Na, E.S., Los, M.F., Cheng, P.F., Kavalali, E.T., and Monteggia, L.M. (2011). NMDA receptor blockade at rest triggers rapid behavioural antidepressant responses. Nature *475*, 91–95.
18. Molendijk, M.L., and de Kloet, E.R. (2022). Forced swim stressor: Trends in usage and mechanistic consideration. Eur. J. Neurosci. *55*, 2813–2831.
19. Riehl, R., Kyzar, E., Allain, A., Green, J., Hook, M., Monnig, L., Rhymes, K., Roth, A., Pham, M., Razavi, R., et al. (2011). Behavioral and physiological effects of acute ketamine exposure in adult zebrafish. Neurotoxicol. Teratol. *33*, 658–667.
20. Burgstaller, J., Hindinger, E., Donovan, J., Maschio, M.D., Kist, A.M., Gesierich, B., Portugues, R., and Baier, H. (2019). Light-sheet imaging and graph analysis of antidepressant action in the larval zebrafish brain network. bioRxiv, 618843. https://doi.org/10.1101/618843.
21. Berman, R.M., Cappiello, A., Anand, A., Oren, D.A., Heninger, G.R., Charney, D.S., and Krystal, J.H. (2000). Antidepressant effects of ketamine in depressed patients. Biol. Psychiatry *47*, 351–354.
22. Li, N., Lee, B., Liu, R.-J., Banasr, M., Dwyer, J.M., Iwata, M., Li, X.-Y., Aghajanian, G., and Duman, R.S. (2010). mTOR-dependent synapse formation underlies the rapid antidepressant effects of NMDA antagonists. Science *329*, 959–964.
23. Sleigh, J., Harvey, M., Voss, L., and Denny, B. (2014). Ketamine – More mechanisms of action than just NMDA blockade. Tren. Anaesth. Crit. Care *4*, 76–81.
24. Casarotto, P.C., Girych, M., Fred, S.M., Kovaleva, V., Moliner, R., Enkavi, G., Biojone, C., Cannarozzo, C., Sahu, M.P., Kaurinkoski, K., et al. (2021). Antidepressant drugs act by directly binding to TRKB neurotrophin receptors. Cell *184*, 1299–1313.e19.
25. Ma, S., Chen, M., Jiang, Y., Xiang, X., Wang, S., Wu, Z., Li, S., Cui, Y., Wang, J., Zhu, Y., et al. (2023). Sustained antidepressant effect of ketamine through NMDAR trapping in the LHb. Nature *622*, 802–809.
26. Davoudian, P.A., Shao, L.-X., and Kwan, A.C. (2023). Shared and Distinct Brain Regions Targeted for Immediate Early Gene Expression by Ketamine and Psilocybin. ACS Chem. Neurosci. *14*, 468–480.
27. López-Gil, X., Jiménez-Sánchez, L., Campa, L., Castro, E., Frago, C., and Adell, A. (2019). Role of Serotonin and Noradrenaline in the Rapid Antidepressant Action of Ketamine. ACS Chem. Neurosci. *10*, 3318–3326.
28. Traber, D.L., and Wilson, R.D. (1969). Involvement of the sympathetic nervous system in the pressor response to ketamine. Anesth. Analg. *48*, 248–252.
29. Stenovec, M., Li, B., Verkhratsky, A., and Zorec, R. (2020). Astrocytes in rapid ketamine antidepressant action. Neuropharmacology *173*, 108158.
30. Warden, M.R., Selimbeyoglu, A., Mirzabekov, J.J., Lo, M., Thompson, K.R., Kim, S.-Y., Adhikari, A., Tye, K.M., Frank, L.M., and Deisseroth, K. (2012). A prefrontal cortex-brainstem neuronal projection that controls response to behavioural challenge. Nature *492*, 428–432.
31. Yang, Y., Cui, Y., Sang, K., Dong, Y., Ni, Z., Ma, S., and Hu, H. (2018). Ketamine blocks bursting in the lateral habenula to rapidly relieve depression. Nature *554*, 317–322.
32. Cui, Y., Yang, Y., Ni, Z., Dong, Y., Cai, G., Foncelle, A., Ma, S., Sang, K., Tang, S., Li, Y., et al. (2018). Astroglial Kir4.1 in the lateral habenula drives neuronal bursts in depression. Nature *554*, 323–327.
33. Zhou, X., Zhao, C., Xu, H., Xu, Y., Zhan, L., Wang, P., He, J., Lu, T., Gu, Y., Yang, Y., et al. (2024). Pharmacological inhibition of Kir4.1 evokes rapid-onset antidepressant responses. Nat. Chem. Biol. *20*, 857–866. https://doi.org/10.1038/s41589-024-01555-y.
34. Kokkinou, M., Ashok, A.H., and Howes, O.D. (2018). The effects of ketamine on dopaminergic function: meta-analysis and review of the implications for neuropsychiatric disorders. Mol. Psychiatry *23*, 59–69.
35. Datta, M.S., Chen, Y., Chauhan, S., Zhang, J., De La Cruz, E.D., Gong, C., and Tomer, R. (2023). Whole-brain mapping reveals the divergent impact of ketamine on the dopamine system. Cell Rep. *42*, 113491.
36. Wu, M., Minkowicz, S., Dumrongprechachan, V., Hamilton, P., Xiao, L., and Kozorovitskiy, Y. (2021). Attenuated dopamine signaling after aversive learning is restored by ketamine to rescue escape actions. eLife *10*, e64041. https://doi.org/10.7554/eLife.64041.
37. Wu, M., Minkowicz, S., Dumrongprechachan, V., Hamilton, P., and Kozorovitskiy, Y. (2021). Ketamine Rapidly Enhances Glutamate-Evoked Dendritic Spinogenesis in Medial Prefrontal Cortex Through Dopaminergic Mechanisms. Biol. Psychiatry *89*, 1096–1105.
38. Lasič, E., Lisjak, M., Horvat, A., Božić, M., Šakanović, A., Anderluh, G., Verkhratsky, A., Vardjan, N., Jorgačevski, J., Stenovec, M., et al. (2019). Astrocyte Specific Remodeling of Plasmalemmal Cholesterol Composition by Ketamine Indicates a New Mechanism of Antidepressant Action. Sci. Rep. *9*, 10957.
39. Yuan, J., Zhang, Y., Yang, H., Cao, S., Luo, Y., and Yu, T. (2023). Astrocytes Are Involved in the Effects of Ketamine on Synaptic Transmission in Rat Primary Somatosensory Cortex. J. Integr. Neurosci. *22*, 116.
40. Ardalan, M., Rafati, A.H., Nyengaard, J.R., and Wegener, G. (2017). Rapid antidepressant effect of ketamine correlates with astroglial plasticity in the hippocampus. Br. J. Pharmacol. *174*, 483–492.
41. Murphy-Royal, C., Ching, S., and Papouin, T. (2023). A conceptual framework for astrocyte function. Nat. Neurosci. *26*, 1848–1856.
42. Diaz Verdugo, C., Myren-Svelstad, S., Aydin, E., Van Hoeymissen, E., Deneubourg, C., Vanderhaeghe, S., Vancraeynest, J., Pelgrims, R., Cosacak, M.I., Muto, A., et al. (2019). Glia-neuron interactions underlie state transitions to generalized seizures. Nat. Commun. *10*, 3830.
43. Reitman, M.E., Tse, V., Mi, X., Willoughby, D.D., Peinado, A., Aivazidis, A., Myagmar, B.-E., Simpson, P.C., Bayraktar, O.A., Yu, G., et al. (2023). Norepinephrine links astrocytic activity to regulation of cortical state. Nat. Neurosci. *26*, 579–593. https://doi.org/10.1038/s41593-023-01284-w.
44. Ollivier, M., Soto, J.S., Linker, K.E., Moye, S.L., Jami-Alahmadi, Y., Jones, A.E., Divakaruni, A.S., Kawaguchi, R., Wohlschlegel, J.A., and Khakh, B.S. (2024). Crym-positive striatal astrocytes gate perseverative behaviour. Nature *627*, 358–366.

45. Peng, L., Verkhratsky, A., Gu, L., and Li, B. (2015). Targeting astrocytes in major depression. Expert Rev. Neurother. *15*, 1299–1306.

46. Cao, X., Li, L.-P., Wang, Q., Wu, Q., Hu, H.-H., Zhang, M., Fang, Y.-Y., Zhang, J., Li, S.-J., Xiong, W.-C., et al. (2013). Astrocyte-derived ATP modulates depressive-like behaviors. Nat. Med. *19*, 773–777.

47. Wang, Q., Jie, W., Liu, J.-H., Yang, J.-M., and Gao, T.-M. (2017). An astroglial basis of major depressive disorder? An overview. Glia *65*, 1227–1250.

48. González-Arias, C., Sánchez-Ruiz, A., Esparza, J., Sánchez-Puelles, C., Arancibia, L., Ramírez-Franco, J., Gobbo, D., Kirchhoff, F., and Perea, G. (2023). Dysfunctional serotonergic neuron-astrocyte signaling in depressive-like states. Mol. Psychiatry *28*, 3856–3873. https://doi.org/10.1038/s41380-023-02269-8.

49. Paukert, M., Agarwal, A., Cha, J., Doze, V.A., Kang, J.U., and Bergles, D.E. (2014). Norepinephrine controls astroglial responsiveness to local circuit activity. Neuron *82*, 1263–1270.

50. Ma, Z., Stork, T., Bergles, D.E., and Freeman, M.R. (2016). Neuromodulators signal through astrocytes to alter neural circuit activity and behaviour. Nature *539*, 428–432.

51. Bekar, L.K., He, W., and Nedergaard, M. (2008). Locus coeruleus alpha-adrenergic-mediated activation of cortical astrocytes in vivo. Cereb. Cortex *18*, 2789–2795.

52. Ding, F., O'Donnell, J., Thrane, A.S., Zeppenfeld, D., Kang, H., Xie, L., Wang, F., and Nedergaard, M. (2013). α1-Adrenergic receptors mediate coordinated Ca2+ signaling of cortical astrocytes in awake, behaving mice. Cell Calcium *54*, 387–394.

53. Yang, E., Zwart, M.F., James, B., Rubinov, M., Wei, Z., Narayan, S., Vladimirov, N., Mensh, B.D., Fitzgerald, J.E., and Ahrens, M.B. (2022). A brainstem integrator for self-location memory and positional homeostasis in zebrafish. Cell *185*, 5011–5027.e20.

54. Domino, E.F., and Chodoff, P. (1965). Pharmacologic effects of CI-581, a new dissociative anesthetic, in man. Clin Pharmacol Ther. *6*, 279–291.

55. Morrison, J.H., Molliver, M.E., and Grzanna, R. (1979). Noradrenergic innervation of cerebral cortex: widespread effects of local cortical lesions. Science *205*, 313–316.

56. Oyarzabal, E.A., Hsu, L.-M., Das, M., Chao, T.-H.H., Zhou, J., Song, S., Zhang, W., Smith, K.G., Sciolino, N.R., Evsyukova, I.Y., et al. (2022). Chemogenetic stimulation of tonic locus coeruleus activity strengthens the default mode network. Sci. Adv. *8*, eabm9898.

57. Winchenbach, J., Düking, T., Berghoff, S.A., Stumpf, S.K., Hülsmann, S., Nave, K.-A., and Saher, G. (2016). Inducible targeting of CNS astrocytes in Aldh1l1-CreERT2 BAC transgenic mice. F1000Res 5, 2934.

58. Gu, X., Zhao, Z., Chen, X., Zhang, L., Fang, H., Zhao, T., Ju, S., Gao, W., Qian, X., Wang, X., et al. (2023). Imaging microglia surveillance during sleep-wake cycles in freely behaving mice. Elife *12*, e86749. https://doi.org/10.7554/eLife.86749.

59. Gregus, A., Wintink, A.J., Davis, A.C., and Kalynchuk, L.E. (2005). Effect of repeated corticosterone injections and restraint stress on anxiety and depression-like behavior in male rats. Behav. Brain Res. *156*, 105–114.

60. Holsboer, F. (2000). The Corticosteroid Receptor Hypothesis of Depression. Neuropsychopharmacology *23*, 477–501.

61. Kim, J.-W., Kleinfelter, B., Kavalali, E.T., and Monteggia, L.M. (2024). Distinct synaptic mechanisms drive the behavioral response to acute stress and rapid correction by ketamine. Neuropsychopharmacology *49*, 1916–1924.

62. Iijima, M., Ito, A., Kurosu, S., and Chaki, S. (2010). Pharmacological characterization of repeated corticosterone injection-induced depression model in rats. Brain Res. *1359*, 75–80.

63. Luo, S., Wu, F., Fang, Q., Hu, Y., Zhang, H., Yuan, S., Yang, C., Shi, Y., and Luo, Y. (2024). Antidepressant effect of teriflunomide via oligodendrocyte protection in a mouse model. Heliyon *10*, e29481. https://doi.org/10.1016/j.heliyon.2024.e29481.

64. McLean, T.H., Parrish, J.C., Braden, M.R., Marona-Lewicka, D., Gallardo-Godoy, A., and Nichols, D.E. (2006). 1-Aminomethylbenzocycloalkanes: conformationally restricted hallucinogenic phenethylamine analogues as functionally selective 5-HT2A receptor agonists. J. Med. Chem. *49*, 5794–5803.

65. Hibicke, M., Landry, A.N., Kramer, H.M., Talman, Z.K., and Nichols, C.D. (2020). Psychedelics, but Not Ketamine, Produce Persistent Antidepressant-like Effects in a Rodent Experimental System for the Study of Depression. ACS Chem. Neurosci. *11*, 864–871.

66. de la Fuente Revenga, M., Zhu, B., Guevara, C.A., Naler, L.B., Saunders, J.M., Zhou, Z., Toneatti, R., Sierra, S., Wolstenholme, J.T., Beardsley, P.M., et al. (2021). Prolonged epigenomic and synaptic plasticity alterations following single exposure to a psychedelic in mice. Cell Rep. *37*, 109836.

67. Cameron, L.P., Tombari, R.J., Lu, J., Pell, A.J., Hurley, Z.Q., Ehinger, Y., Vargas, M.V., McCarroll, M.N., Taylor, J.C., Myers-Turnbull, D., et al. (2021). A non-hallucinogenic psychedelic analogue with therapeutic potential. Nature *589*, 474–479.

68. Kaplan, A.L., Confair, D.N., Kim, K., Barros-Álvarez, X., Rodriguiz, R.M., Yang, Y., Kweon, O.S., Che, T., McCorvy, J.D., Kamber, D.N., et al. (2022). Bespoke library docking for 5-HT2A receptor agonists with antidepressant activity. Nature *610*, 582–591.

69. Dong, C., Ly, C., Dunlap, L.E., Vargas, M.V., Sun, J., Hwang, I.-W., Azinfar, A., Oh, W.C., Wetsel, W.C., Olson, D.E., et al. (2021). Psychedelic-inspired drug discovery using an engineered biosensor. Cell *184*, 2779–2792.e18.

70. Mitchell, P.J., and Redfern, P.H. (1992). Acute and chronic antidepressant drug treatments induce opposite effects in the social behaviour of rats. J. Psychopharmacol. *6*, 241–257.

71. Mombereau, C., Gur, T.L., Onksen, J., and Blendy, J.A. (2010). Differential effects of acute and repeated citalopram in mouse models of anxiety and depression. Int. J. Neuropsychopharmacol. *13*, 321–334.

72. Raison, C.L., Sanacora, G., Woolley, J., Heinzerling, K., Dunlop, B.W., Brown, R.T., Kakar, R., Hassman, M., Trivedi, R.P., Robison, R., et al. (2023). Single-Dose Psilocybin Treatment for Major Depressive Disorder: A Randomized Clinical Trial. JAMA *330*, 843–853.

73. Davis, A.K., Barrett, F.S., May, D.G., Cosimano, M.P., Sepeda, N.D., Johnson, M.W., Finan, P.H., and Griffiths, R.R. (2021). Effects of Psilocybin-Assisted Therapy on Major Depressive Disorder: A Randomized Clinical Trial. JAMA Psychiatry *78*, 481–489.

74. Goodwin, G.M., Aaronson, S.T., Alvarez, O., Arden, P.C., Baker, A., Bennett, J.C., Bird, C., Blom, R.E., Brennan, C., Brusch, D., et al. (2022). Single-Dose Psilocybin for a Treatment-Resistant Episode of Major Depression. N. Engl. J. Med. *387*, 1637–1648.

75. Rinaman, L. (2011). Hindbrain noradrenergic A2 neurons: diverse roles in autonomic, endocrine, cognitive, and behavioral functions. Am. J. Physiol. Regul. Integr. Comp. Physiol. *300*, R222–R235.

76. Randlett, O., Wee, C.L., Naumann, E.A., Nnaemeka, O., Schoppik, D., Fitzgerald, J.E., Portugues, R., Lacoste, A.M.B., Riegler, C., Engert, F., et al. (2015). Whole-brain activity mapping onto a zebrafish brain atlas. Nat. Methods *12*, 1039–1046.

77. Gigliucci, V., O'Dowd, G., Casey, S., Egan, D., Gibney, S., and Harkin, A. (2013). Ketamine elicits sustained antidepressant-like activity via a serotonin-dependent mechanism. Psychopharmacology *228*, 157–166.

78. Feng, J., Zhang, C., Lischinsky, J.E., Jing, M., Zhou, J., Wang, H., Zhang, Y., Dong, A., Wu, Z., Wu, H., et al. (2019). A Genetically Encoded Fluorescent Sensor for Rapid and Specific In Vivo Detection of Norepinephrine. Neuron *102*, 745–761.e8.

79. Wan, J., Peng, W., Li, X., Qian, T., Song, K., Zeng, J., Deng, F., Hao, S., Feng, J., Zhang, P., et al. (2021). A genetically encoded sensor for measuring serotonin dynamics. Nat. Neurosci. *24*, 746–752.

80. Uribe-Arias, A., Rozenblat, R., Vinepinsky, E., Marachlian, E., Kulkarni, A., Zada, D., Privat, M., Topsakalian, D., Charpy, S., Candat, V., et al.

(2023). Radial astrocyte synchronization modulates the visual system during behavioral-state transitions. Neuron *111*, 4040–4057.e6.

81. Klapoetke, N.C., Murata, Y., Kim, S.S., Pulver, S.R., Birdsey-Benson, A., Cho, Y.K., Morimoto, T.K., Chuong, A.S., Carpenter, E.J., Tian, Z., et al. (2014). Independent optical excitation of distinct neural populations. Nat. Methods *11*, 338–346.
82. Chen, S., Chiu, C.N., McArthur, K.L., Fetcho, J.R., and Prober, D.A. (2016). TRP channel mediated neuronal activation and ablation in freely behaving zebrafish. Nat. Methods *13*, 147–150.
83. Thrane, A.S., Rangroo Thrane, V., Zeppenfeld, D., Lou, N., Xu, Q., Nagelhus, E.A., and Nedergaard, M. (2012). General anesthesia selectively disrupts astrocyte calcium signaling in the awake mouse cortex. Proc. Natl. Acad. Sci. USA *109*, 18974–18979.
84. Vesuna, S., Kauvar, I.V., Richman, E., Gore, F., Oskotsky, T., Sava-Segal, C., Luo, L., Malenka, R.C., Henderson, J.M., Nuyujukian, P., et al. (2020). Deep posteromedial cortical rhythm in dissociation. Nature *586*, 87–94.
85. Hirschfeld, R.M. (2000). History and evolution of the monoamine hypothesis of depression. J. Clin. Psychiatry *61*, 4–6.
86. Monai, H., Ohkura, M., Tanaka, M., Oe, Y., Konno, A., Hirai, H., Mikoshiba, K., Itohara, S., Nakai, J., Iwai, Y., et al. (2016). Calcium imaging reveals glial involvement in transcranial direct current stimulation-induced plasticity in mouse brain. Nat. Commun. *7*, 11100.
87. Rush, A.J., Marangell, L.B., Sackeim, H.A., George, M.S., Brannan, S.K., Davis, S.M., Howland, R., Kling, M.A., Rittberg, B.R., Burke, W.J., et al. (2005). Vagus nerve stimulation for treatment-resistant depression: a randomized, controlled acute phase trial. Biol. Psychiatry *58*, 347–354.
88. Krahl, S.E., Senanayake, S.S., Pekary, A.E., and Sattin, A. (2004). Vagus nerve stimulation (VNS) is effective in a rat model of antidepressant action. J. Psychiatr. Res. *38*, 237–240.
89. Chen, A.B., Duque, M., Wang, V.M., Dhanasekar, M., Mi, X., Rymbek, A., Tocquer, L., Narayan, S., Prober, D., Yu, G., et al. (2024). Norepinephrine changes behavioral state via astroglial purinergic signaling. Preprint at bioRxiv. https://doi.org/10.1101/2024.05.23.595576.
90. Xin, Q., Wang, J., Zheng, J., Tan, Y., Jia, X., Ni, Z., Feng, J., Wu, Z., Li, Y., Li, X., et al. (2024). Neuron-astrocyte Coupling in Lateral Habenula Mediates Depressive-like Behaviors. Preprint at bioRxiv. https://doi.org/10.1101/2024.11.03.621722.
91. Colucci, W.S., and Alexander, R.W. (1986). Norepinephrine-induced alteration in the coupling of alpha 1-adrenergic receptor occupancy to calcium efflux in rabbit aortic smooth muscle cells. Proc. Natl. Acad. Sci. USA *83*, 1743–1746.
92. Stenovec, M., Božić, M., Pirnat, S., and Zorec, R. (2020). Astroglial Mechanisms of Ketamine Action Include Reduced Mobility of Kir4.1-Carrying Vesicles. Neurochem. Res. *45*, 109–121. https://doi.org/10.1007/s11064-019-02744-1.
93. Rihel, J., Prober, D.A., Arvanites, A., Lam, K., Zimmerman, S., Jang, S., Haggarty, S.J., Kokel, D., Rubin, L.L., Peterson, R.T., et al. (2010). Zebrafish behavioral profiling links drugs to biological targets and rest/wake regulation. Science *327*, 348–351.
94. Dunn, T.W., Mu, Y., Narayan, S., Randlett, O., Naumann, E.A., Yang, C.-T., Schier, A.F., Freeman, J., Engert, F., and Ahrens, M.B. (2016). Brain-wide mapping of neural activity controlling zebrafish exploratory locomotion. eLife *5*, e12741.
95. Antinucci, P., Dumitrescu, A., Deleuze, C., Morley, H.J., Leung, K., Hagley, T., Kubo, F., Baier, H., Bianco, I.H., and Wyart, C. (2020). A calibrated optogenetic toolbox of stable zebrafish opsin lines. eLife *9*, e54937. https://doi.org/10.7554/eLife.54937.
96. Dana, H., Mohar, B., Sun, Y., Narayan, S., Gordus, A., Hasseman, J.P., Tsegaye, G., Holt, G.T., Hu, A., Walpita, D., et al. (2016). Sensitive red protein calcium indicators for imaging neural activity. eLife *5*, e12727. https://doi.org/10.7554/eLife.12727.
97. Friard, O., and Gamba, M. (2016). BORIS: a free, versatile open-source event-logging software for video/audio coding and live observations. Methods Ecol. Evol. *7*, 1325–1330.
98. Deng, F., Wan, J., Li, G., Dong, H., Xia, X., Wang, Y., Li, X., Zhuang, C., Zheng, Y., Liu, L., et al. (2023). Dual-color GRAB sensors for monitoring spatiotemporal serotonin release in vivo. Preprint at bioRxiv. https://doi.org/10.1101/2023.05.27.542566.
99. Kim, Y.S., Anderson, M., Park, K., Zheng, Q., Agarwal, A., Gong, C., Saijilafu, Y., Young, L., He, S., LaVinka, P.C., et al. (2016). Coupled Activation of Primary Sensory Neurons Contributes to Chronic Pain. Neuron *91*, 1085–1096.
100. White, R.M., Sessa, A., Burke, C., Bowman, T., LeBlanc, J., Ceol, C., Bourque, C., Dovey, M., Goessling, W., Burns, C.E., et al. (2008). Transparent adult zebrafish as a tool for in vivo transplantation analysis. Cell Stem Cell *2*, 183–189.
101. Urasaki, A., Asakawa, K., and Kawakami, K. (2008). Efficient transposition of the Tol2 transposable element from a single-copy donor in zebrafish. Proc. Natl. Acad. Sci. USA *105*, 19827–19832.
102. Bahl, A., and Engert, F. (2020). Neural circuits for evidence accumulation and decision making in larval zebrafish. Nat. Neurosci. *23*, 94–102.
103. Dubbs, A., Guevara, J., and Yuste, R. (2016). moco: Fast Motion Correction for Calcium Imaging. Front. Neuroinform. *10*, 6.
104. Kalman, R.E. (1960). A new approach to linear filtering and prediction problems. J. Basic Eng. *82*, 35–45.

Please cite this article in press as: Duque et al., Ketamine induces plasticity in a norepinephrine-astroglial circuit to promote behavioral perseverance, Neuron (2024), https://doi.org/10.1016/j.neuron.2024.11.011

STAR★METHODS

KEY RESOURCES TABLE

REAGENT or RESOURCE	SOURCE	IDENTIFIER
Chemicals, peptides, and recombinant proteins		
MS-222 (Tricaine methanesulfonate)	Sigma Aldrich	Cat#E10521
Ketamine hydrochloride	Patterson Veterinary	Cat#07-803-6637
Dextromethorphan hydrobromide	Sigma Aldrich	Cat#D9684
D(-)-2-Amino-5-phosphonopentanoic acid (AP-5)	Sigma Aldrich	Cat#A8054
MK-801 maleate	Cayman Chemicals	Cat#10009019
Fluoxetine hydrochloride	Sigma Aldrich	Cat#F132
Escitalopram oxalate	Sigma Aldrich	Cat#E4786
Desipramine hydrochloride	Sigma Aldrich	Cat#D3900
TCB-2	Cayman Chemicals	Cat#2592
Memantine hydrochloride	Sigma Aldrich	Cat#M9292
DOI hydrochloride	Sigma Aldrich	Cat#D101
Prazosin hydrochloride	Sigma Aldrich	Cat#P7791
Hydrocortisone - Water Soluble	Sigma Aldrich	Cat#H0396
Capsaicin	Sigma Aldrich	Cat#M2028
Dexamethasone	VetOne	Cat#13985-037-02
Dexmedetomidine	Precedex	Cat#10010202
Tamoxifen	Sigma Aldrich	Cat#T5648
R-69 hydrochloride	Kaplan et al.[68] Roth Lab	N/A
Tabernanthalog (TBG) fumarate	Cameron et al.[67] Olson Lab	N/A
AAZ hydrochloride	Dong et al.[69] Olson Lab	N/A
Experimental models: Organisms/strains		
Zebrafish: Tg(gfap:jRGECO1a)	Mu et al.[9]	N/A
Zebrafish: Tg(elavl3:H2B-jGCaMP7f)^{jf90}	Dunn et al.[94]	N/A
Zebrafish: Tg(dbh:KalTA4);Tg(UAS:CoChR-eGFP)	Antinucci et al.[95]	N/A
Zebrafish: Tg(gfap:TRPV1-T2A-eGFP)^{jf64}	This paper	N/A
Zebrafish: Tg(elavl3:GRABNE$_{2h}$)	This paper	N/A
Zebrafish: Tg(elavl3:GRAB$_{5\text{-}HT2.0}$)	This paper	ZFIN ct876Tg
Mouse: Tg(Aldh1l1-CreER;GCaMP6s)	Dr. Gesine Saher, Winchenbach et al.[57]	N/A
Mouse: Tg(Thy1-jRGECO1a)	The Jackson Laboratory	RRID:IMSR_JAX:030526
Software and algorithms		
Bigstream	Greg M. Fleishman	https://github.com/JaneliaSciComp/bigstream
GraphPad Prism	GraphPad	RRID:SCR_002798
Voluseg	Mu et al.[9,96]	https://github.com/mikarubi/voluseg
Fiji (Imaging Analysis)	NIH	RRID:SCR_003070
BORIS	Friard et al.[97]	https://www.boris.unito.it/
Custom Python scripts	This study	https://doi.org/10.5281/zenodo.14174436
ZBrain	Randlett et al.[76]	https://zebrafishexplorer.zib.de/home/

Please cite this article in press as: Duque et al., Ketamine induces plasticity in a norepinephrine-astroglial circuit to promote behavioral perseverance, Neuron (2024), https://doi.org/10.1016/j.neuron.2024.11.011

EXPERIMENTAL MODEL AND STUDY PARTICIPANT DETAILS

Larval zebrafish

Experiments were conducted according to the guidelines of the National Institutes of Health and were approved by the Standing Committee on the Use of Animals in Research of Harvard University. Animals were handled according IACUC protocols #1836 (Prober lab), 22-0216 (Ahrens lab), #2729 (Engert lab) and 18-11-340-1 (Fishman lab). For all experiments in larval zebrafish, we used wild-type larval zebrafish (strains AB, WIK or TL), aged 5–8 days post-fertilization (dpf). We did not determine the sex of the fish we used since it is indeterminate at this age. Fish were raised in shallow Petri dishes and fed ad libitum with paramecia after 4 dpf. Fish were raised on a 14 h:10 h light:dark cycle at around 27°C. All experiments were done during daylight hours (4–14 h after lights on). All protocols and procedures were approved by the Harvard University/Faculty of Arts and Sciences Standing Committee on the Use of Animals in Research and Teaching (Institutional Animal Care and Use Committee), and the Janelia Institutional Animal Care and Use Committee.

For all behavioral experiments we used:

Wild type - strains AB and WIK

For imaging of astroglial calcium we used:

Cytosolic, red calcium indicator. *Tg(gfap:jRGECO1a)*[9,96]

For imaging of neuronal calcium we used:

Nuclear-localized, green calcium indicator. *Tg(elavl3:H2B-jGCaMP7f)*^{jf90} [94]

For optogenetic activation of norepinephrinergic neurons we used:

Channelrhodopsin expressed under dbh promoter. *Tg(dbh:KalTA4);Tg(UAS:CoChR-eGFP)*[95]

For chemogenetic activation of astroglia we used:

Rat transient receptor potential cation channel subfamily V member 1 (TRPV1) expressed under *gfap* promoter. *Tg(gfap:TRPV1-T2A-eGFP)*^{jf64} (*this paper*)

For imaging extracellular norepinephrine concentrations we used:

$GRAB_{NE2h}$[78] green fluorescent extracellular norepinephrine sensor expressed under *elavl3* promoter. *Tg(elavl3:*$GRAB_{NE2h}$*)* (*this paper*).

For imaging extracellular serotonin concentrations we used:

$GRAB_{5\text{-}HT2.0}$[98] green fluorescent extracellular serotonin sensor expressed under *elavl3* promoter. *Tg(elavl3:*$GRAB_{5\text{-}HT2.0}$*)* (ZFIN ct876Tg) (*this paper*).

Mice

For mouse experiments, female and male adult mice were used and randomly assigned to experimental groups. There was no influence or association of sex on the findings. All mice were healthy, and none were excluded from the analysis. Mice were maintained on a 12-hour light/dark cycle, housed in groups no larger than five, and received food and water ad libitum. All mouse experiments were conducted in accordance with the National Institute of Health Guide for the Care and Use of Laboratory Animals and protocols approved by the Animal Care and Use Committee at Johns Hopkins University.

For astrocyte imaging experiments during tail suspension test and ketamine injection we used:

Aldh1l1-CreER;GCaMP6s[57,99] transgenic mice

For neuronal imaging experiments we used:

Thy1-jRGECO1a (RRID:IMSR_JAX:030526) transgenic mice

METHOD DETAILS

Zebrafish transgenesis

We generated the *Tg(gfap:TRPV1-T2A-eGFP)*^{jf64}, *Tg(elavl3:*$GRAB_{NE2h}$*)*and *Tg(elavl3:*$GRAB_{5\text{-}HT2.0}$*)* lines used in this paper. The lines were generated in a casper background[100] using the Tol2 method.[101]

Embedding of larval zebrafish for tail-tracking experiments

Larval zebrafish aged 6-8 dpf were embedded in small round Petri dishes (e.g. Corning #351006); importantly, dishes should not be tissue culture-treated to allow agarose to adhere. Solutions of 2% low melting-point agarose (Sigma-Aldrich A9414) were prepared by heating powdered agarose in system water and agitating until solution was clear. The 2% agarose solution was kept at 42-48 degrees Celsius. To embed fish, a small amount of 2% agarose solution was pipetted in the middle of a Petri dish. A larval zebrafish was then transferred, using either a small glass or Pasteur pipette, taking care to minimize addition of water to the agarose solution during transfer. Using either small forceps or a small (~10-100 μL) plastic micropipette tip, larval zebrafish were gently rotated until they were dorsal side up. Fish often struggle when transferred to the agarose solution, so care should be taken to keep fish righted until agarose solidifies. Once the agarose solidified, we freed the tail of the fish by carefully cutting away the hardened agarose around the tail with a micro-scalpel (Fine Science Tools 10315-12). Care should be taken to remove enough agarose to prevent the tail from hitting or becoming stuck on agarose during swimming or struggle.

Please cite this article in press as: Duque et al., Ketamine induces plasticity in a norepinephrine-astroglial circuit to promote behavioral perseverance, Neuron (2024), https://doi.org/10.1016/j.neuron.2024.11.011

Pharmacological treatment of larval zebrafish

Approximately 10-20 larval zebrafish aged 6-8 dpf were transferred to single wells in 12-well plates containing 2 mL of fish water (8-12 fish/well). Quantities of either the experimental pharmacological compound (Table S1) or vehicle control were added and fish were incubated for one hour. Fish were then washed three times in a larger Petri dish and then allowed to recover for one hour, following which experimentation would begin. In the case of the hydrocortisone treatment, fish were incubated for 48h from 5dpf to 7dpf and kept in hydrocortisone water during experimentation. For the MS-222 experiments, to avoid pH effects, the solution was buffered with 10mM HEPES and pH adjusted to 6.8-7.4 using a 1M solution of NaOH.

For Figure 1E and all other imaging experiments, fish were first embedded in agarose as described above and then treated with either the pharmacological compound or vehicle control.

Tail-tracking of embedded larval zebrafish and visual stimulus

For all behavioral experiments involving embedded larval zebrafish, we used a previously published, custom-build behavioral rig and custom-written code.[102] Briefly, we illuminated the fish and its environment using infrared light-emitting diode panels (wavelength 940 nm, Cop Security). The tail-posture of the fish was tracked using a camera (Grasshopper3-NIR, FLIR Systems) with a zoom lens (Zoom 7000, 18–108 mm, Navitar) and a long-pass filter (R72, Hoya). We determined the posture of the tail, as well as its tip angle, by analyzing the position of ~25 equally spaced, user-defined key points along its length. Posture was determined and recorded in real-time at 90 Hz using custom-written Python scripts (Python 3.7, OpenCV 4.1). Tail vigor was calculated as the standard deviation of the tail angle, using a 500 ms rolling window. The visual stimuli consisted of gratings (bright and dark bars, ~10 mm wide) underneath that could be moved forward or backward relative to the fish. The code for the specific protocol used during the giving up assay can be found in GitHub (https://doi.org/10.5281/zenodo.14174436).

Tracking of freely swimming larval zebrafish

For all behavioral experiments involving freely-swimming larval zebrafish (Figures S1C, S1F, and S1G), we also used a previously published, custom-build behavioral rig and custom-written code.[102] The illumination and detection of freely swimming fish used the same behavioral rigs as described for embedded fish. To track the position of fish and determine swim bouts in real time at 90 Hz, we used custom-written Python scripts (Python 3.7, OpenCV 4.1). The background of the camera image was subtracted and the body of the fish identified by center of mass. Orientation was determined as the axis of largest pixel variance in the identified body. Swim bouts were detected by computing a 50-ms rolling variance and identifying thresholded peaks.

Passivity computation in zebrafish

Passive periods were operationally defined to be periods greater than 10 s in length in which the fish did not perform a swim bout. To determine the percentage of the open-loop interval spent passive per trial, the total length of all passive periods within the open-loop interval of a trial was summed and the sum divided by the length of the open-loop interval. The same computation was performed to determine passive fraction for closed-loop intervals as well. To account for variability between different clutches, open-loop passivity was normalized to vehicle-treated controls from the same clutch (Norm. passivity). Raw passivity values were provided for Figures 1 and 2H for illustrative purposes.

Epifluorescence imaging of neurons and radial astrocytes in embedded larval zebrafish

Larval zebrafish aged 6-8 dpf were embedded in small round petri dishes and their tails freed as described previously. To image neurons, we used previously published fish lines (see Fish Lines section) *Tg(elavl3:H2B-GCaMP7f)* for neural imaging and *Tg(gfap:jRGECO1a)* for astroglial imaging. Imaging was performed using a dissecting microscope (Olympus MVX10) with a CMOS camera (IDS Imaging UI-3370CP-NIR) and an LED lamp for fluorescent imaging (X-Cite 120 LED mini). For analysis, each video frame was registered to a reference brain using OpenCV and fluorescence in each defined brain region was extracted with manually segmented masks. Fluorescence Z-score was calculated as the difference between mean total fluorescence before treatment subtracted to average baseline fluorescence, divided by the standard deviation of total fluorescence before treatment, for each mask.

Confocal imaging of extracellular norepinephrine and astroglial calcium in zebrafish

Larval zebrafish aged 6-8 dpf of the line *Tg(elavl3:GRAB$_{NE2h}$);Tg(gfap:jRGECO1a)* were embedded in small round petri dishes and their tails freed as described previously. Two-color imaging was performed at 0.5 Hz using a Zeiss LSM 980 NLO confocal microscope (488 and 561 nm laser illumination) with a 20x magnification objective (Zeiss #421452-9800-000). Ketamine (200 mg/L) was added to the bath with a 200 μL micropipette at 100 frames. For experiments in which prazosin was added prior to imaging, fish were incubated in prazosin (100 μM in bath) for at least 2 h before embedding. For experiments in which MS-222 was added prior to imaging, fish were incubated in MS-222 (150 mg/L) for at least 30 min prior to imaging. Fluorescence was extracted with manually segmented masks. For each fish, the same mask was used for the green and red channels. ΔF/F calculations were performed as described above.

Fictive behavior in virtual reality and light-sheet imaging in zebrafish

The setup used for fictive behavior during light-sheet imaging was adapted from Mu et al.[9], using a single laser beam and illumination objective. Animals in fictive-behavior experiments for light-sheet imaging were not paralyzed. Fish were directly transferred to an acrylic pedestal in a custom-fabricated sample holder with glass windows allowing side illumination and immobilized with 2% agarose. Agarose was removed by hand over a small square in the tail to allow access for the electrodes while still restricting overall movement, and agarose was removed around the head to minimize aberration of the light-sheet illumination of the brain. One suction electrode (~60 μm inner diameter) filled with external solution, was placed over the dorsal side of the fish's tail and attached with gentle negative pressure. The voltage signal recorded by this tail was amplified and filtered (band-pass 300 Hz - 3 kHz) with a MultiClamp 700B amplifier. This signal was then smoothed through convolution with an exponential filter and used as the 'swim signal'.

For the struggle analysis performed in Figures 8 and S8, we first detected swims by detecting peaks in the swim signal (minimum inter-peak interval > 500 ms). We then z-scored swim amplitudes and manually set a z-score threshold for each fish, above which a swim would be classified as a struggle. The same set of z-score thresholds were used to analyze neural and glial activity.

Analysis of zebrafish light-sheet calcium imaging data

We extracted cell segments from raw fluorescence data with a volumetric segmentation pipeline available from https://github.com/mikarubi/voluseg, and described previously.[9,53] We calculated ΔF/F for each cell segment using a 100s rolling baseline window as described in Yang et al..[53] For the acute ketamine imaging, we calculated the $\log_2$ fold change for each cell segment as:

$$log_2FC = log_2\left(\frac{Average\ \Delta F/F_{After\ ketamine}}{Average\ \Delta F/F_{Before\ ketamine}}\right)$$

For the activation-inhibition maps, we sorted cell segments according to the fold change and plotted the top 5% most activated and inhibited segments, for each fish.

For the fictive behavior calcium imaging data, we ran the segmentation and obtained ΔF/F for each cell segment as described above.

For the statistical analysis across atlas brain regions for Figure 4, we bootstrapped a 95% confidence interval in shuffled data by shuffling the brain area ID corresponding to each segmented unit, then taking the top 5% of shuffled units to calculate a mean activation for each brain region. This was repeated separately for all fish, then a mean taken across fish to complete a single bootstrap trial. We repeated the bootstrapping process 10,000 times, then took the 2.5 and 97.5 percentiles to generate the confidence interval.

Registration of different zebrafish brain volumes and Z-Brain masks

To compare results across fish we registered all experiments to a representative brain volume, using BigStream (https://github.com/JaneliaSciComp/bigstream).

For the light-sheet calcium imaging data, after registration of all experimental volumes together, we registered a Z-Brain reference H2B-mCherry volume[76] to the representative brain volume and applied the same transformation to previously defined reference masks (total of 294 masks) for every brain region.

Optogenetic and chemogenetic activation experiments in zebrafish

For the optogenetic experiments, *Tg(dbh:KalTA4);Tg(UAS:CoChR-eGFP)*[81,95] fish were incrossed and their larvae raised until 6-8 dpf. Fish were screened using an epifluorescence scope and selected according to the GFP signal in NE-MO cells, and raised to 6-8 dpf. Positive fish were then placed on top of a 16x16 blue LED matrix and stimulated for 30 minutes with blue light (0.3W, Newegg #9SIA9DCJ4V0029) or control ambient light. After 1h recovery, fish were assayed in our futility-induced passivity test. For the imaging experiments, positive fish also expressing *Tg(gfap:jRGECO1a)* were imaged in a confocal microscope and stimulated from the top using a blue light (450-460nm) LED source (UltraFire #WF-508BL) for 5 seconds.

For the chemogenetic experiments, *Tg(gfap:TRPV1-T2A-eGFP)*^{jf64} were crossed with WT fish from a casper background. Fish were screened using an epifluorescence scope and selected according to the GFP signal in hindbrain and spinal cord glia, and raised to 6-8 dpf. Positive fish were then incubated with 2μM capsaicin (Sigma #12084) in fish water (0.025% DMSO final concentration) or an equivalent concentration of vehicle for 20-30 minutes. Fish were then washed and placed in fresh fish water. After 1h recovery, fish were assayed in our futility-induced passivity test.

Tamoxifen preparation and induction in mouse

Conditional knockin Rosa26-lsl-GCaMP6s[99] and Aldh1l1-CreER[57] mouse lines have been previously described. To induce GCaMP6s expression in *Aldh1l1-CreER;GCaMP6s* transgenic mice, tamoxifen (TAM) (Sigma-Aldrich, T5648) was freshly prepared on the first day of the injection at 10 mg/mL in sunflower seed oil (Sigma-Aldrich, S5007) through intermittent sonication at room temperature (RT). Adult (> 6 weeks) mice were injected intraperitoneally (i.p.) with a dosage of 100 mg/kg body weight (b.w.) for five consecutive days, once per day. Every injection was at least 20 hours (hrs) apart. The remaining tamoxifen solution was stored at 4℃ in the dark for a maximum of 5 days. All experiments were performed at least 2 weeks after the last tamoxifen injection.

Please cite this article in press as: Duque et al., Ketamine induces plasticity in a norepinephrine-astroglial circuit to promote behavioral perseverance, Neuron (2024), https://doi.org/10.1016/j.neuron.2024.11.011

Head plate installation and cranial window surgery in mouse

The day before cranial window surgery, dexamethasone (VetOne, NDC#13985-037-02) was given through drinking water to the mice (1 mg/kg) that completed TAM administration (see above). The next day, animals were anesthetized with inhaled isoflurane (0.25-5%) and placed in a custom-made stereotaxic frame. Surgery was performed under standard and sterile conditions. After hair removal and lidocaine application (1%, VetOne, NDC 13985-222-04), the mouse's skull surrounding the left retrosplenial cortex was exposed and the connective tissue was carefully removed. VetbondTM (3M) was used to close the incision site. A custom-made metal head plate was fixed to the cleaned skull using dental cement (C&B Metabond, Parkell Inc.). A 3-mm diameter circular craniotomy was then performed using a high-speed dental drill bit. The center of the craniotomy was located 1 mm lateral to lambda. Dura was left intact and the cranial window was then sealed with a custom-made 3 mm diameter circular #1 (0.17 mm) coverslip using VetbondTM. A layer of cyanoacrylate (Krazy Glue) was applied on top of the Vetbond to secure the coverslip. Animals recovered in their home cages for at least 2 weeks before imaging.

In vivo 2P imaging during tail suspension

For two-photon microscopy of tail suspension, a miniature two-photon microscope (FHIRM-TPM V2.0, Field of view: 190 3 190 mm2; Resolution: 650 nm; working distance: 400 mm) was employed. Imaging data were acquired using the imaging software (GINKGO-MTPM, Transcend Vivoscope Biotech Co., Ltd, China) at a frame rate of 9.57 Hz (440 x 380 pixels) with a femtosecond fiber laser (920 nm, 35 mW at the objective, TVS-FL-01, Transcend Vivoscope Biotech Co., Ltd, China). A webcam was used to capture the behavioral data at 25 Hz. Mice were habituated to the weight of the fiber over the course of one week prior to tail suspension. For the tail suspension, mouse was suspended by its tail from a rod suspended 20 cm above the table with adhesive tape placed 1 cm. Mice were suspended for a total of 7 minutes, and the time where the animal remained immobile was quantified over the last 6 minutes of the recording.

In vivo 2P laser scanning microscopy and ketamine delivery for astrocyte Ca^{2+} activity in mouse

Two-photon laser scanning microscopy was performed with a Zeiss LSM 710 microscope equipped with a GaAsP detector, which uses a mode-locked Ti-Sapphire laser (Coherent Chameleon Ultra II) tuned to 920 nm. The head of the mouse was immobilized by attaching the head plate to a custom-made stage mounted on a vibration isolation table, and the body of the mouse was housed in a custom-made plastic restrainer. Images were collected 100 – 150 mm below dura using a coverslip-corrected Zeiss 20x/1.0 W Plan-Apochromat objective with a pixel dwelling time of 1.58 ms and scanning speed of 2 Hz. Mice were kept on the stage for no more than two hours and all *in vivo* imaging experiments were performed during the day.

For *in vivo* ketamine delivery, an I.P. catheter was inserted into the lower right quadrant of the animal's abdomen (DDP Medical, Cat. 405311). Animals were then imaged as described above. Within 15-30 minutes of the initiating imaging, animals were injected intraperitoneally with ketamine (20 mg/kg; MWIAH; dissolved in 0.9% NaCl) or vehicle (0.9% NaCl). In experiments with α2-adrenergic agonist, 20 mg/kg ketamine was co-administered with dexmedetomidine (0.01 mg/kg; PRECEDEX).

Analysis of mouse imaging data

2P images were motion corrected using moco,[103] and background noise was filtered with a Kalman filter.[104] $\Delta F/F$ was calculated across the whole field as well as individual astrocyte cell bodies by defining F0 as the bottom 10th percentile of intensities prior to ketamine administration. For tail suspension experiments, F0 was defined as the bottom 10th percentile of intensities across the entire imaging session. Animal behavior during tail suspension were scored manually using BORIS.[97]

QUANTIFICATION AND STATISTICAL ANALYSIS

Statistical analyses were performed in GraphPad Prism. When comparing two groups, we used two-tailed t-test for normally distributed data, and two-sided Mann-Whitney rank test otherwise. For multiple group comparisons, we used one-way or two-way ANOVA, followed by multi-comparison test. Exact p values are reported in the figure legends, along with the sample number for each group and statistical test description. All results were represented as mean ± SEM.